Exelon Generation

200 Exelon Way
Kennett Square, PA 19348
www.exeloncorp.com

PROPRIETARY INFORMATION – WITHHOLD UNDER 10 CFR 2.390

10 CFR 50.55a

December 20, 2021

U.S. Nuclear Regulatory Commission
Attn: Document Control Desk
Washington, DC 20555-0001

Peach Bottom Atomic Power Station, Unit 2
Renewed Facility Operating License No. DPR-44
NRC Docket No. 50-277

Subject: Proposed Relief Request Associated with Reactor Pressure Vessel N-16A Nozzle Repair

Reference: 1) Letter from J. Danna (U.S. Nuclear Regulatory Commission) to D. Rhoades (Exelon Generation Company, LLC), "Peach Bottom Atomic Power Station, Unit No. 2 - Approval of One-Time Alternative to Flaw Characterization and Removal Requirements for N-16A Nozzle (EPID L-2020-LLR-0144)," dated April 23, 2021 (ML21110A680)

In accordance with 10 CFR 50.55a, "Codes and standards," paragraph (z)(2), Exelon Generation Company, LLC (EGC) requests approval of the attached relief request associated with the repair of a 2-inch instrument line nozzle at penetration N-16A on the Reactor Pressure Vessel (RPV). A relief request concerning this nozzle repair was previously approved in the Reference 1 letter for one operating cycle. The attached relief request applies to the remainder of the fifth 10-year Inservice Inspection (ISI) interval and the remainder of the plant life, which is currently scheduled to conclude on August 8, 2053.

The fifth 10-year ISI interval for Peach Bottom Atomic Power Station (PBAPS), Unit 2 began on January 1, 2019 and will conclude December 31, 2028. The fifth 10-year ISI interval complies with the American Society of Mechanical Engineers (ASME) Boiler and Pressure Vessel Code, Section XI, 2013 Edition.

We request your approval by October 3, 2022 in support of the Fall 2022 Unit 2 Refueling Outage.

A summary of the regulatory commitments contained in this submittal is provided in Attachment 1. Attachment 2 contains Relief Request I5R-14, Revision 1. Attachments 3, 4, and 5 contain information proprietary to the Framatome Inc. (Framatome). Framatome requests that Attachments 3, 4, and 5 be withheld from public disclosure in accordance with 10 CFR 2.390. Attachments 6, 7, and 8 contain non-proprietary versions of the documents. Affidavits supporting this request are contained in Attachments 9, 10, and 11.

If you have any questions or require additional information, please contact Tom Loomis at 610-765-5510.

Respectfully,

D. P. Helker

David P. Helker
Senior Manager - Licensing & Regulatory Affairs
Exelon Generation Company, LLC

Attachments:
1) Summary of Commitments
2) Relief Request I5R-14, Revision 1
3) "Peach Bottom Unit 2 RV Instrument Nozzle N16A Repair As-Left J-Groove Weld Analysis," Framatome Document No. 32-9335342-000, Proprietary Version
4) "Peach Bottom Unit 2 RV Instrument Nozzle N16A Repair Weld Residual Stress Analysis," Framatome Document No. 32-9334548-000, Proprietary Version
5) "Corrosion Evaluation of the Peach Bottom Unit 2 N16-A Reactor Vessel Nozzle Modification," Framatome Document No. 51-9320932-002, Proprietary Version
6) "Peach Bottom Unit 2 RV Instrument Nozzle N16A Repair As-Left J-Groove Weld Analysis - Non Proprietary," Framatome Document No. 32-9337878-000, Non-Proprietary Version
7) "Peach Bottom Unit 2 RV Instrument Nozzle N16A Repair Weld Residual Stress Analysis – Non Proprietary" Framatome Document No. 32-9337544-000, Non-Proprietary Version
8) "Corrosion Evaluation of the Peach Bottom Unit 2 N16-A Reactor Vessel Nozzle Modification – Non Proprietary," Framatome Document No. 51-9321006-002, Non-Proprietary Version
9) Affidavit Associated with Framatome Document No. 32-9335342-000
10) Affidavit Associated with Framatome Document No. 32-9334548-000
11) Affidavit Associated with Framatome Document No. 51-9320932-002

cc: USNRC Region I, Regional Administrator
USNRC Senior Resident Inspector, PBAPS
USNRC Project Manager, PBAPS
W. DeHass, Pennsylvania Bureau of Radiation Protection (w/o Attachments)

ATTACHMENT 1

Summary of Commitments

Attachment 1
Summary of Commitments

The following table identifies commitments made in this document. (Any other actions discussed in the submittal represent intended or planned actions. They are described to the NRC for the NRC's information and are not regulatory commitments.)

COMMITMENT	**COMMITTED DATE OR "OUTAGE"**	**COMMITMENT TYPE**	
		ONE-TIME ACTION (Yes/No)	**Programmatic (Yes/No)**
EGC will perform a bare metal VT-2 examination of the N-16A location from the OD of the PBAPS, Unit 2 vessel.	Each refueling outage during the Class 1 System Leakage Test.	No	Yes
EGC will perform a best-effort UT of the RPV low alloy steel surrounding the Unit 2 N-16A penetration to confirm that the as-left j-groove weld flaw does not propagate into the vessel wall material.	During the next refueling outage (P2R24 (2022)) and every 10 years thereafter.	No	Yes

Attachment 2

Peach Bottom Atomic Power Station, Unit 2
Proposed Relief Request Associated with Reactor Pressure Vessel Nozzle Repair
Relief Request I5R-14, Revision 1

1. ASME CODE COMPONENTS AFFECTED

Code Class:	1
Reference:	IWB-2500, Table IWB-2500-1
Exam Category:	B-P
Item Number:	B15.10
Description:	Reactor Pressure Vessel (RPV) Instrument Penetration – 2-inch Nominal Pipe Size
Component Number:	N-16A

2. APPLICABLE CODE EDITION AND ADDENDA

The current Edition for the Inservice Inspection (ISI) interval is the American Society of Mechanical Engineers (ASME) Code, Section XI, 2013 Edition. The code of construction for the RPV is the ASME Code Section III, 1965 Edition with Addenda to and including Winter 1965 Addenda.

3. APPLICABLE CODE REQUIREMENT

Flaw Removal

- IWA-5250(a)(3) states "Components requiring corrective action shall have repair/replacement activities performed in accordance with IWA-4000 or corrective measures performed where the relevant condition can be corrected without a repair/replacement activity."

- IWA-4412 states "Defect removal shall be accomplished in accordance with the requirements of IWA-4420."

- IWA-4611.1(a) states "Defects shall be removed in accordance with IWA-4422.1. A defect is considered removed when it has been reduced to an acceptable size."

- N-528 of Section III, 1965 Edition with Addenda to and including Winter 1965, requires repair of weld defects including removal of defects detected by leakage tests.

Flaw Evaluation

- IWB-3522.1 states, in part, "A component whose visual examination (IWA-5240) detects any of the following relevant conditions shall meet IWB-3142 and IWA-5250 prior to continued service ... "

- IWB-3142.1(b) states "A component whose visual examination detects the relevant conditions described in the standards of Table IWB-3410-1 shall be unacceptable for continued service, unless such components meet the requirements of IWB-3142.2, IWB-3142.3, or IWB-3142.4."

- IWA-3300(a) states, in part, "Flaws detected by the preservice and inservice examinations shall be sized ... "

- IWA-3300(b) states, in part, "Flaws shall be characterized in accordance with IWA-3310 through IWA-3390, as applicable ... "

- IWB-3610(b) states, in part, "For purposes of evaluation by analysis, the depth of flaws in clad components shall be defined in accordance with Fig. IWB-3610-1 ... "

- The implementing reply of N-749 states “It is the opinion of the Committee that, in lieu of IWB-3610 and IWB-3620, flaws in ferritic steel components operating in the upper shelf temperature range may be evaluated using the following acceptance criteria.” The methods and criteria of N-749 are based on the methods of elastic-plastic fracture mechanics (EPFM).

- IWB-3420 states "Each detected flaw or group of flaws shall be characterized by the rules of IWA-3300 to establish the dimensions of the flaws. These dimensions shall be used in conjunction with the acceptance standards of IWB-3500."

4. REASON FOR REQUEST

Following a routine refueling outage on October 29, 2020, leakage was observed between the RPV wall and the N-16A, a 2-inch water level instrument line nozzle, during the pre-startup system leakage testing of the Peach Bottom Atomic Power Station (PBAPS), Unit 2 RPV (See Enclosure 1).

As a result of leakage indications on the RPV penetration N-16A, Exelon Generation Company, LLC (EGC) performed a half-nozzle repair which partially replaced the existing nozzle assembly with a nozzle penetration that is resistant to Intergranular Stress Corrosion Cracking (IGSCC).

EGC applied a welded pad on the Outer Diameter (OD) of the RPV using IGSCC resistant nickel Alloy 52M (ERNiCrFe-7A) filler metal. The new weld pad was installed using a machine Gas Tungsten Arc Welding (GTAW) Ambient Temperature Temper Bead (ATTB) welding technique. Then, EGC attached an IGSCC resistant nozzle to the new weld pad with a partial penetration weld using a non-temper bead manual welding technique and IGSCC resistant nickel Alloy 52M filler metal.

The original partial penetration attachment weld and a remnant of the original nozzle remains in place. A one-cycle flaw evaluation was performed to demonstrate the acceptability of leaving the original partial penetration attachment weld, with a maximum postulated flaw, in place for one cycle. NRC approval was sought and received for one cycle via Safety Evaluation dated April 23, 2021 (Reference ML21110A680). In Revision 1 of this relief request, approval is being requested for the proposed alternatives which now includes a multi-cycle flaw evaluation (see "Flaw Analytical Evaluation" below). Additionally, IWA-4412 and IWA-4611 contain requirements for the removal of, or reduction in size of, defects. The defect on N-16A was not removed; therefore, relief is also sought from these requirements.

IWB-3400 and IWB-3600 were written with the expectation that volumetric Non-Destructive Examination (NDE) techniques such as Ultrasonic Testing (UT) would be used to determine the flaw size and shape. In support of the flaw evaluation, the ASME Code paragraphs IWB-3420 and IWB-3610(b) require characterization of the flaw in the N-16A penetration. Although demonstrated, there is not a Performance Demonstration Initiative (PDI) qualified technique to perform NDE of the partial penetration weld in this configuration that can be used to accurately characterize the location, orientation, or size of a flaw in the weld.

The flaw evaluation methods presented in IWB-3610 and Appendix A of Section XI are based on Linear Elastic Fracture Mechanics (LEFM) methods. Code Case N-749 was developed to provide criteria for the use of Elastic-Plastic Fracture Mechanics methods (EPFM) as acceptable alternatives to the LEFM methods currently contained in IWB-3610 and Appendix A, for operating conditions where ferritic vessel materials are operating on the material toughness upper shelf. This Code Case is Conditionally Accepted in Revision 19 of NRC Regulatory Guide 1.147.

NB-4620 requires all welds to be post-weld heat treated except as otherwise permitted in NB-4622.7. Relief was initially requested and approved to install a welded pad using ATTB welding in accordance with ASME Code Case N-638-7. The NRC has conditionally approved ASME Code Case N-638-7 to allow ATTB welding of dissimilar materials.

5. PROPOSED ALTERNATIVES AND BASIS FOR USE

In accordance with 10 CFR 50.55a, "Codes and standards," paragraph (z)(2), EGC proposes the following alternatives to the requirements specified in Section 3 above on the basis that performing a Code required repair results in a hardship without a compensating increase in quality and safety. A repair in accordance with the ASME Code, which would remove the flaw from the inner portion of the vessel, would require a full core offload to access the repair location, result in significant risk associated with the inclusion of loose parts and foreign material, and result in significant increase in radiological exposure. These areas of concern result in a significant hardship over the installed repair. In lieu of the ASME Code compliant repair, the following alternatives are proposed:

- As an alternative to flaw removal or reduction in size to meet the applicable acceptance standards per IWA-4412 and IWA-4611, EGC has implemented an OD repair of the RPV instrument nozzle N-16A utilizing an OD weld pad and half nozzle as described in the repair of nozzle penetration section below.

- As an alternative to performing the NDE required to characterize the flaw under IWB-3420 and IWB-3610(b) in penetration N-16A, EGC analyzed a maximum postulated flaw that bounds the range of flaw sizes that could exist in the original J-groove weld and nozzle.

- As an alternative to NB-4620, EGC installed a welded pad using ATTB welding in accordance with ASME Code Case N-638-7. The NRC has conditionally approved ASME Code Case N-638-7 to allow ATTB welding of dissimilar materials.

Basis for Use

A. Background

The PBAPS, Unit 2 RPV is manufactured from SA-302, Grade B, modified by ASME Code Case 1339 Paragraph 1, steel that is ID clad with stainless steel. The reactor vessel water instrument nozzles are fabricated with Alloy 600 material (SB-166). See Enclosure 1 for a sketch of N-16A.

During refueling outage P2R23 (2020), EGC discovered a leak at the instrument penetration nozzle N-16A located on the RPV. Visual examination detected active leakage at the nozzle interface (annular gap) with the RPV OD during the Class 1 system leakage test. EGC performed a half-nozzle repair at the N-16A location based on the discussion provided in the following sections.

B. Cause of Leakage

After discovery of the leak from the RPV OD, an EVT-1 visual examination was performed of the N-16A wetted surfaces from the inside diameter (ID) of the RPV with a color camera. The internal visual examination did identify an apparent surface crack approximately 1.15” in length at the 6 o’clock position extending radially from the inside edge of the Alloy 600 nozzle into the Alloy 182 J-groove weld. This surface crack’s location is consistent with the location of leakage observed on the exterior of the RPV at the N-16A nozzle during the bare metal visual leakage inspection (VT-2).

After completion of the internal visual exam, a nozzle plug with a face plate seal was installed in the inside diameter of the N-16A nozzle to facilitate the half nozzle repair (see Enclosure 2). Following plug installation, no leakage was observed coming through or around the nozzle and a demonstrated volumetric ultrasonic examination (UT) was performed from the RPV exterior surface for informational purposes (see "Examination of the J-groove Weld" below).

During the UT examination, a single planar radial-axial indication was detected and noted to be present throughout the entire J-groove cross sectional area, but no penetration into the ferritic vessel base metal was detected. The ultrasonic indication was located at the nozzle 6 o’clock position, which correlates to the reported flaw location from the visual examinations. In addition, no circumferential indications in either the J-groove weld or adjacent low alloy steel base material were detected. The ultrasonic inspection report also noted that the weld image showed the J-groove weld at a larger depth into the RPV base material than the 9/16 inch minimum specified in the design drawing. This could be indicative that a repair(s) was made to this weld during fabrication, though no fabrication records have been found that confirm this possibility.

The combined and spatially correlated internal and external visual and ultrasonic results suggest that the most probable cause of the external leakage observed coming from the N-16A nozzle is that a single radial-axial oriented IGSCC flaw initiated in the J-groove weld and then propagated through the J-groove weld until it reached a depth where a leak path in the annulus between the nozzle and reactor vessel penetration existed.

A search of fabrication records for the N-16A nozzle and J-groove weld has not identified any anomalous material conditions or process deviations that could have contributed to the IGSCC indication observed; however, it is possible that subsurface fabrication defects could have existed to further propagate the flaw through the J-groove weld.

C. Extent of Condition

The leakage between the RPV wall and the N-16A instrument nozzle was identified during the Class 1 system leakage test. As part of the Class 1 system leakage test, a bare metal VT-2 was performed on the five other additional RPV instrument nozzles (N-11A, N-11B, N-12A, N-12B, and N-16B), and there was no evidence of leakage on any of the nozzles during examination.

D. Examination of the J-groove Weld

A visual examination was performed from the RPV ID using a color camera at the N-16A location. The exam volume encompassed the Alloy 182 J-groove weld, outer portions of the Alloy 600 nozzle bore, and the inside surface of the RPV immediately adjacent to the N-16A location. The visual examination was performed before and after the area was hydrolazed. The visual examination revealed a surface crack at the 6 o'clock position beginning on the vertical nozzle face and extending down the wall approximately 1.15 inches. The indication does not appear to extend beyond the radius into the horizontal portion of the nozzle bore.

A volumetric (UT) examination was performed on the N-16A J-groove weld from the RPV OD in accordance with BWRVIP-03, Rev. 19. This examination was conducted to supplement visual examinations performed from the RPV ID. This volumetric examination technique has been demonstrated to provide crack detection, length sizing, and depth sizing of flaws that initiate within the partial penetration J-groove weld material and to detect planar flaw indications in the low alloy vessel material, but has not been qualified in accordance with ASME Section XI, Appendix VIII. The exam volume included the J-groove weld and the RPV low alloy steel interface. The UT exam identified one flaw indication in the J-groove weld material recorded in both the clockwise and counterclockwise scan directions. The position of the flaw was in the same area as recorded during the visual examination from the RPV ID. No reflectors extending into the RPV base material were observed; thus, this UT exam provides reasonable confidence that the flaw has not propagated into the RPV low alloy steel.

E. Flaw Analytical Evaluation

A flaw evaluation was performed as provided in Attachment 3. Additionally, in support of the flaw evaluation, a weld residual stress analysis was performed as provided in Attachment 4. The postulated flaw is shown to be acceptable after the installation of the modification.

F. Repair of Nozzle Penetration

EGC replaced the existing N-16A nozzle assembly during P2R23 (Fall 2020 refueling outage) with a new half-nozzle penetration that is resistant to IGSCC, which meets ASME Section XI and Code Case N-638-7 as was conditionally approved by the NRC in Regulatory Guide 1.147, Revision 19 and ASME Section III. See Enclosure 2 for a sketch of the RPV instrument nozzle repair. A welded pad was applied to the OD of the RPV using IGSCC resistant nickel Alloy 52M filler metal and was welded using the machine GTAW ATTB welding technique. The IGSCC resistant nozzle was attached to the new weld pad with a partial penetration weld using a non-temper bead manual welding technique and IGSCC resistant filler metal. The original partial penetration attachment weld and a remnant of the original nozzle remains in place.

A design analysis was performed in accordance with the design requirements of ASME Section III. The analysis confirmed that the new nozzle will not eject from the RPV under design conditions. The new design was reconciled to the original construction code and addresses design and transient loads to ensure all Code requirements were met.

The accumulated Effective Full Power Years (EFPYs) for PBAPS, Unit 2, was 35.64 at the time of the repair, but the fluence analysis used a conservative value of 35.7 EFPY. The fast neutron fluence value (E > 1.0 MeV) at 35.7 EFPY for the N-16A nozzle at the outside diameter (1T) is 5.45E+16 neutrons/cm^2. This value used the DPA-weighted attenuation method as described in Regulatory Guide 1.99, and is below the threshold level of 1E+17 neutrons/cm^2 (E > 1.0 MeV). The material in the area of this repair is not expected to have decreased fracture toughness or ductility associated with damage of low alloy steels in the beltline region; therefore, there is not a weldability concern for the repair.

G. Corrosion Evaluation

A corrosion evaluation was performed to consider potential material degradation due to the repair of the N-16A RPV instrumentation nozzle (Attachment 5). The corrosion evaluation concludes that the modification of the N-16A RPV nozzle, which exposes the low alloy steel RPV to a water environment and introduced new materials (Alloy 690 and Alloy 52M), is acceptable.

H. Loose Parts Evaluations

Given the original N-16A nozzle was not entirely removed, EGC completed a lost-parts evaluation to assess the potential for nozzle segments to enter the RPV during power operation. Two evaluations were completed to address the potential impact on the fuel and the potential impact on internal RPV components. The evaluations determined that the potential for lost parts did not pose any safety concerns. The evaluations considered interfacing systems and other RPV internal components, flow blockage, and adverse chemical reactions.

I. Follow-up Examinations

EGC will perform a bare metal VT-2 examination of the N-16A location from the OD of the vessel each Unit 2 refueling outage during the Class 1 System Leakage Test. Additionally, EGC will perform a best-effort UT of the RPV low alloy steel surrounding the Unit 2 N-16A penetration during the next refueling outage and every 10 years thereafter to confirm that the as-left j-groove weld flaw does not propagate into the vessel wall material. These commitments are discussed in Attachment 1, “Summary of Commitments.”

Conclusion

Based on the above, in accordance with 10 CFR 50.55a(z)(2), EGC has concluded that performing a Code required repair results in a hardship without a compensating increase in quality and safety.

6. DURATION OF PROPOSED ALTERNATIVE

The attached relief request applies to the remainder of the fifth 10-year ISI interval and the remainder of the plant life, which is currently scheduled to conclude on August 8, 2053.

7. PRECEDENTS

1. Letter from J. Danna (U.S. Nuclear Regulatory Commission) to B. Hanson (Exelon Generation Company, LLC), "Limerick Generating Station, Unit 2 – Issuance of Relief Request IR4-17, Revision 1, RE: Reactor Pressure Vessel Nozzle Repair in Lieu of Specific ASME Code Requirements (EPID L-2018-LLR-0071)," dated March 5, 2019 (ML19009A002)

2. Letter from J. Wiebe (U.S. Nuclear Regulatory Commission) to M. Pacilio (Exelon Generation Company, LLC), "Quad Cities Nuclear Power Station, Unit 2 – Safety Evaluation in Support of Request for Relief Associated with the Reactor Pressure Vessel Nozzle Repairs (TAC NO. ME8347)," dated January 30, 2013 (ML13016A454)

Enclosure 1
N-16A Figure

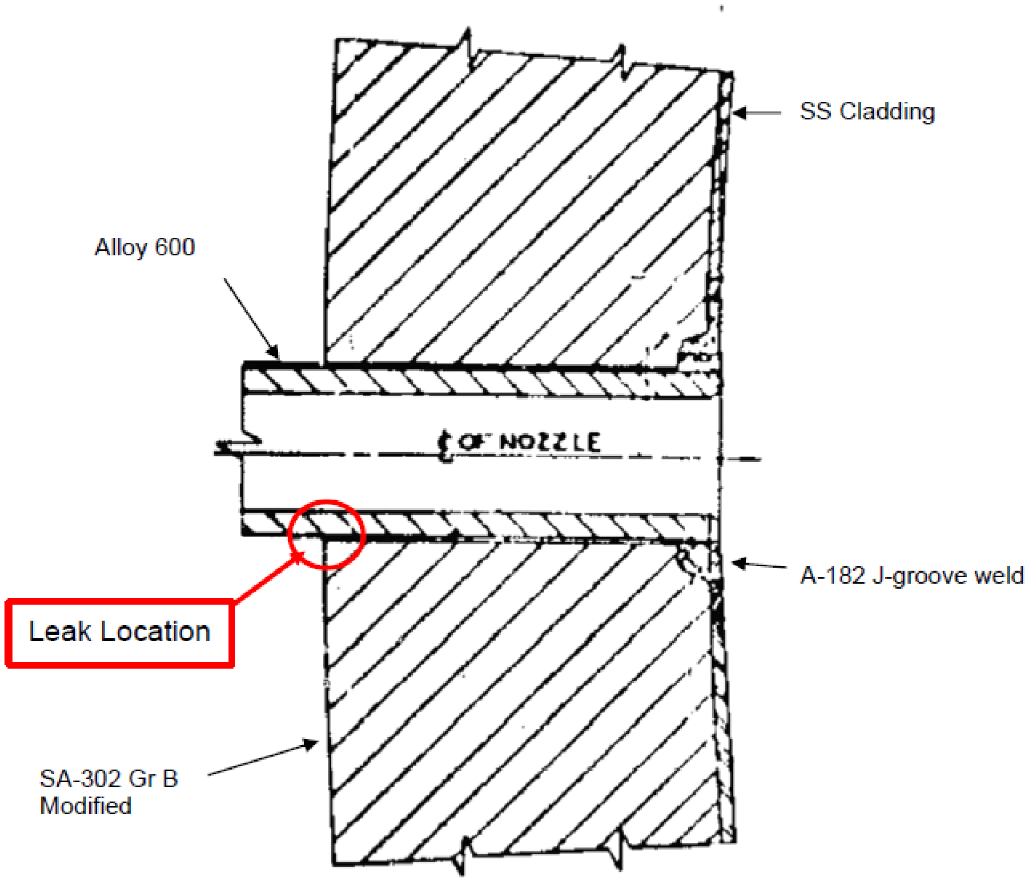

Enclosure 2
Repaired N-16A

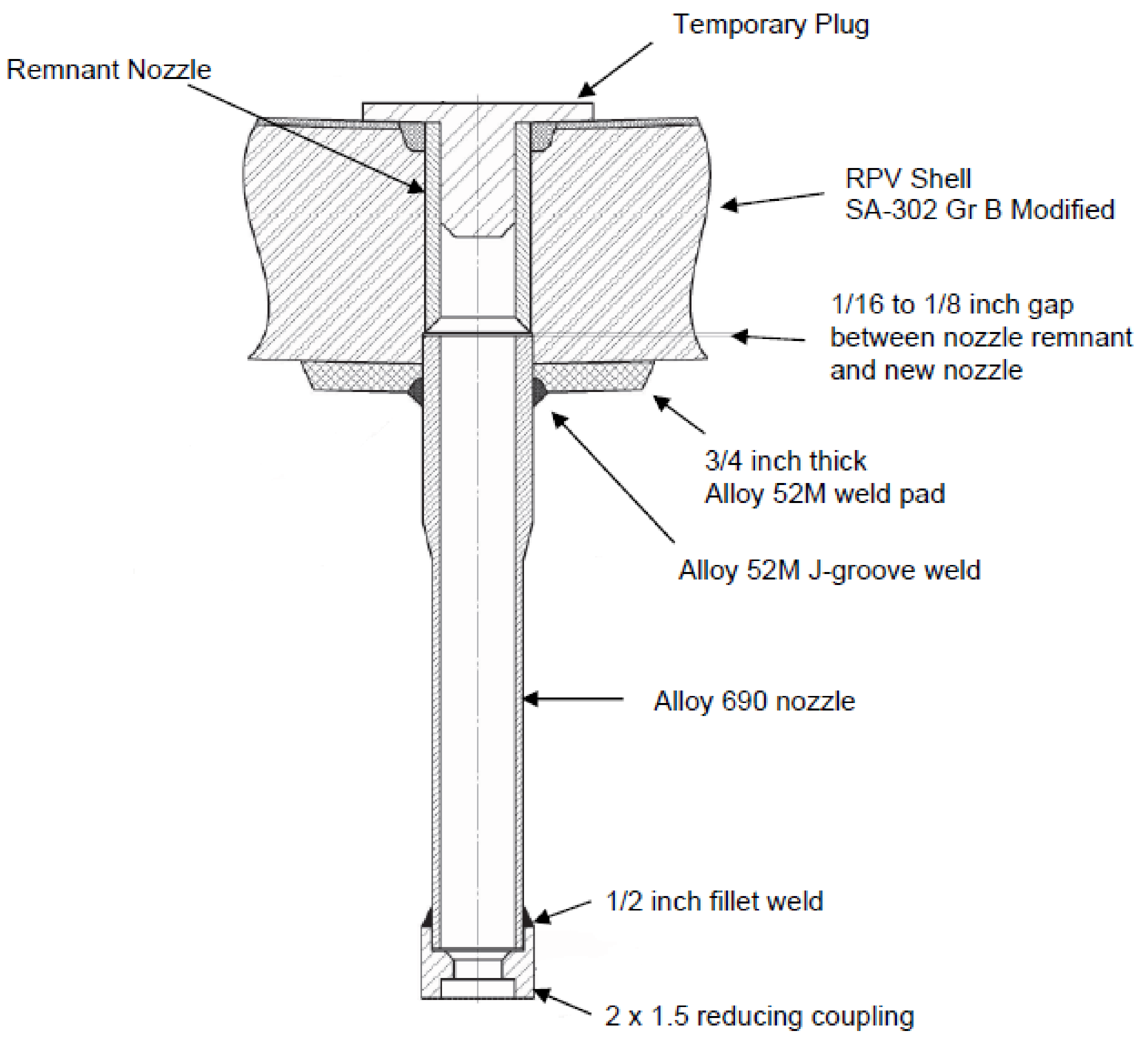

Attachment 3

"Peach Bottom Unit 2 RV Instrument Nozzle N16A Repair As-Left J-Groove Weld Analysis,"
Framatome Document No. 32-9335342-000, Proprietary Version

Attachment 4

"Peach Bottom Unit 2 RV Instrument Nozzle N16A Repair Weld Residual Stress Analysis,"
Framatome Document No. 32-9334548-000, Proprietary Version

Attachment 5

"Corrosion Evaluation of the Peach Bottom Unit 2 N16-A Reactor Vessel Nozzle Modification,"
Framatome Document No. 51-9320932-002, Proprietary Version

Attachment 6

"Peach Bottom Unit 2 RV Instrument Nozzle N16A Repair As-Left J-Groove Weld Analysis - Non Proprietary," Framatome Document No. 32-9337878-000, Non-Proprietary Version framatome

CALCULATION SUMMARY SHEET (CSS)

Document No. 32 - 9337878 - 000

Safety Related: ☒Yes ☐ No

Title Peach Bottom Unit 2 RV Instrument Nozzle N16A Repair As-Left J-Groove Weld Analysis – Non Proprietary

PURPOSE AND SUMMARY OF RESULTS:

Purpose:
The purpose of this analysis is to determine the suitability of leaving a degraded J-Groove weld (JGW) in the Peach Bottom Unit 2 Nuclear Power Plant reactor vessel at instrument nozzle N16A following the repair of the leaking nozzle. A fatigue and stress corrosion cracking (SCC) crack growth and fracture mechanics evaluation of the as-left JGW is performed for a postulated radial-axial corner flaw through the entire JGW to demonstrate that the postulated flaw is acceptable from the time of nozzle repair in 2020 through the end of 80-year operation in 2054. This document complements previous flaw evaluation work that supported a one cycle justification of plant operation (Reference 1).

Summary of Results:
The fatigue and SCC crack growth and fracture mechanics evaluation for a postulated flaw in the as-left JGW demonstrates, based on a combination of linear elastic and elastic-plastic fracture mechanics analyses using the safety factors in Table 2-1, and the applicable J-R Curves from Regulatory Guide 1.161 (Reference 2), that the postulated flaw is acceptable from the time of nozzle repair in 2020 through the end of 80-year operation in 2054. In addition, the primary stress criteria of IWB-3610(d)(2) (Reference 4) and 3.1(c) and 3.2(a)(3) of Code Case N-749 (Reference 5) are satisfied since the limit load analysis shows that the structure does not collapse at a pressure equal to 150% of the Design Pressure.

The proprietary version of this document is 32-9335342-000.

Proprietary information in the document is identified by bold brackets (**[ ]**).

If the computer software used herein is not the latest version per the EASI list, AP 0402-01 requires that justification be provided.

THE FOLLOWING COMPUTER CODES HAVE BEEN USED IN THIS DOCUMENT:

CODE/VERSION/REV	CODE/VERSION/REV
ANSYS v19.2	

THE DOCUMENT CONTAINS ASSUMPTIONS THAT SHALL BE VERIFIED PRIOR TO USE

☐Yes
☒ No

Review Method: ☒ Design Review (Detailed Check)

☐ Alternate Calculation

Does this document establish design or technical requirements? ☐ YES ☒ NO

Does this document contain Customer Required Format? ☐ YES ☒ NO

Signature Block

Name and Title (printed or typed)	Signature	P/R/A/M and LP/LR	Date	Pages/Sections Prepared/Reviewed/Approved
Jennifer A. Nelson Principal Engineer	*JA NELSON 12/10/2021*	LP		All
Ashok Nana Advisory Engineer	*AD NANA 12/10/2021*	M		All
Martin Kolar Principal Engineer	*M KOLAR 12/10/2021*	LR		All
Ryan Hosler Supervisory Engineer	*RS HOSLER 12/10/2021*	A		All

Notes: P/R/A designates Preparer (P), Reviewer (R), Approver (A);
LP/LR designates Lead Preparer (LP), Lead Reviewer (LR);
M designates Mentor (M)

In preparing, reviewing and approving revisions, the lead preparer/reviewer/approver shall use 'All' or 'All except ___' in the pages/sections reviewed/approved. 'All' or 'All except ___' means that the changes and the effect of the changes on the entire document have been prepared/reviewed/approved. It does not mean that the lead preparer/reviewer/approver has prepared/reviewed/approved all the pages of the document.

With Approver permission, calculations may be revised without using the latest CSS form. This deviation is permitted when expediency and/or cost are a factor. Approver shall add a comment in the right-most column that acknowledges and justifies this deviation.

Project Manager Approval of Customer References and/or Customer Formatting (N/A if not applicable)

Name (printed or typed)	Title (printed or typed)	Signature	Date	Comments
Dave Skulina	Project Manager	*DJ SKULINA 12/10/2021*		

Record of Revision

Revision No.	Pages/Sections/Paragraphs Changed	Brief Description / Change Authorization
000	All	Original Release

Table of Contents

Table of Contents
(continued)

Page

List of Tables

List of Tables
(continued)

List of Figures

1.0 INTRODUCTION

Instrument nozzle N16A was found leaking at the Peach Bottom, Unit 2, Reactor Vessel (RV) during the Fall 2020 outage. The cause of the leakage was not determined. However, based upon industry experience, the most likely cause is intergranular stress corrosion cracking through either the [ ] J-Groove weld or the [ ] nozzle. A half nozzle repair was designed in which an outboard portion of the existing nozzle was removed and a replacement nozzle attached to a new [ ] weld pad on the OD of the RV. Due to the emergent nature of the repair, Framatome performed a one-cycle justification for the nozzle repair (Reference 1) to support the Relief Request and subsequent NRC approval for plant restart.

The purpose of this analysis is to determine the suitability of leaving a degraded J-Groove weld (JGW) in the Peach Bottom Unit 2 Nuclear Power Plant reactor vessel at instrument nozzle N16A following the repair of the leaking nozzle per Section 5.4.3 of Reference 3 through the end of 80 year plant operation in 2054. Since a potential flaw in the JGW cannot be sized by currently available nondestructive examination techniques, it is conservatively assumed that the 'as-left' condition of the remaining JGW includes degraded or cracked weld material extending through the entire J-groove weld and Alloy 600 remnant nozzle material.

It is conservatively postulated that a radial-axial corner flaw exists through the entire JGW and would propagate into the low alloy steel reactor vessel material by fatigue crack growth under cyclic loading conditions. Although some investigators have suggested that flaw propagation due to stress corrosion cracking would occur at a higher rate than fatigue, stress corrosion cracking is not deemed a likely growth mechanism under normal conditions as discussed in Section 2.3.2. However, it is not entirely possible to rule out, so it is conservatively included in the present flaw evaluation. The applicable code is *ASME Section XI, 2013 Edition* (Reference 4). If the service life of the component is shown to be limited, an alternate approach of using *ASME Section XI Code Case N-749* (Reference 5) as modified by the Nuclear Regulatory Commission (Reference 6) is used. Acceptance of the postulated flaw is determined based on available fracture toughness or ductile tearing resistance using the safety factors outlined in Table 2-1.

2.0 METHODOLOGY

The analytical methodology for the as-left JGW analysis is outlined below.

2.1 Finite Element Analysis to Obtain Weld Residual plus Transient Operating Stresses

For input into the finite element explicit flaw stress intensity factor analysis, the combined weld residual stress (WRS) plus operating transient stresses are obtained by utilizing the model and results developed in the WRS analysis (Reference [7]). The final simulation provided in the WRS analysis is the welding of the new JGW (NJGW) to the new replacement nozzle and weld pad followed by [ ]

The key operating transients are then applied to the model as listed below. The key operating transients are defined in the one cycle justification analysis (Reference 1) as specified in Section 5.4.3 of Reference 3, and considering the [ ] transient per References 8 and 9.

(1) Thermal Analysis: A thermal transient analysis is performed for each applicable transient [ ]

(2) Structural Analysis: A structural analysis is performed for each applicable transient by [ ]

The sequence of each applicable transient is defined as follows:

i. [ ] of [ ] are simulated at the end of the steady state operating cycles provided in Reference 7, followed by [ ] steady state operating condition [ ]

ii. [ ] for each remaining applicable transient is performed at the end of step (2)i above.

(3) Post-Processing: The combined residual plus operating stresses applicable for evaluating a postulated remnant flaw in the as-left J-groove weld are extracted: [ ]

2.2 Explicit Flaw Finite Element Analysis to Obtain Stress Intensity Factors

A radial-axial flaw is postulated in the J-groove weld (JGW) and remnant Alloy 600 nozzle material to obtain stress intensity factors (SIF) for each loading condition at varying positions along the crack front. Radial is with respect to the nozzle axis extending from the inside corner of the penetration to the interface between the JGW and the RV shell. [ ] Detailed analysis steps are as follows:

1. Finite Element Models: Develop a [ ] finite element crack model [ ] with crack tip elements [ ] capable of representing [ ] flaw depths. [ ]

   The initial flaw size, a_o, is characterized by the [ ] finite element models are then generated, with flaw size increments of [ ] These models are used to obtain SIFs at [ ] positions along the crack front for residual and operating stresses, with crack face pressure.

2. Applied Loads: Develop a [ ] to transfer stresses from the uncracked finite element stress analysis model (Section 2.1, Item (3)) to the crack face of the cracked models. [ ]

3. Stress Intensity Factors: Obtain stress intensity factors (SIF) for each loading condition at varying positions along the crack front [ ] Details of the SIF solutions and plastic zone correction are provided in Sections 2.2.1 and 2.2.2.

2.2.1 Stress Intensity Factor Solutions

The SIFs are calculated at a total of [ ] positions along the crack front starting with position [ ] and going to the [ ]

Stress intensity factors at flaw sizes between the modeled flaw sizes are linearly interpolated. If the flaw size is larger than the largest flaw in the finite element model, the stress intensity factor is extrapolated using the following scaling rule:

$$K_I(a_2) = K_I(a_1)\sqrt{\frac{a_2}{a_1}}$$

Where $K_I(a_1)$ is a known SIF at flaw size a_1 and $K_I(a_2)$ is the desired SIF at flaw size a_2. This approach follows the fundamental expression for the stress intensity factor, $K_I = \sigma\sqrt{\pi a}$, where for a given applied stress and geometry, the stress intensity factor scales with the square root of flaw size.

2.2.2 Plastic Zone Correction

The Irwin plastic zone correction is used to account for a moderate amount of yielding. For plane strain conditions, the correction is (Reference 10, Eq. 2.63):

$$r_y = \frac{1}{6\pi}\left(\frac{K_I(a)}{\sigma_y}\right)^2$$

Where $K_I(a)$ is the stress intensity factor at the actual crack size (a), and σ_y is the material yield strength. The effective crack size, a_e, is calculated as:

$$a_e = a + r_y$$

The stress intensity factor at the effective flaw size is then calculated using the scaling law derived above as:

$$K_I(a_e) = K_I(a)\sqrt{\frac{a_e}{a}}$$

2.3 Flaw Growth Calculation

Calculate fatigue flaw growth as detailed in Section 2.3.1, [ ] for cyclic loading conditions using operational stresses from pressure and thermal loads. Since the stresses used in the fatigue flaw growth analysis are the combined residual plus operating stresses, the effect of the residual stresses on fatigue crack growth is captured by the *R* ratio, or KI_{min}/KI_{max} as the weld residual stress is a steady state secondary stress and has only a mean stress effect. Also, flaw growth due to stress corrosion cracking (SCC) as detailed in Section 2.3.2 is calculated in [ ] The total flaw growth is the combined fatigue and stress corrosion crack growth.

Initial flaw size and shape: For 'non-classical' flaw shapes with stress intensity factors calculated by the finite element method, in order to track the flaw size during fatigue crack growth, any characteristic dimension may be used as the initial flaw size. For this calculation, the initial flaw size (a_i) is chosen to be [ ]

2.3.1 Fatigue Crack Growth

Fatigue crack growth is calculated using the fatigue crack growth rate model from Article A-4300 of ASME Section XI (Reference 4) as follows:

$$\frac{da}{dN} = C_0(\Delta K_I)^n$$

Where ΔK_I is the stress intensity factor range in ksi√in, and da/dN is the crack growth rate in inches/cycle. The crack growth rates for a surface flaw are utilized since the postulated flaw results in the low alloy steel vessel being exposed to the water environment.

The detailed equations for calculating the fatigue crack growth rate are presented as follows.

$\Delta K_I = K_{max} - K_{min}$.

$R = K_{Imin} / K_{Imax}$

If $K_{min} \leq 0$, use $R = 0$.

$0 \leq R \leq 0.25$
- $\Delta K_I < 17.74$
  - $n = 5.95$
  - $S = 1.0$
  - $C_0 = 1.02 \times 10^{-12} S$
- $\Delta K_I \geq 17.74$
  - $n = 1.95$
  - $S = 1.0$
  - $C_0 = 1.01 \times 10^{-7} S$

$0.25 < R < 0.65$
- $\Delta K_I < 17.74\ [(3.75R + 0.06)/(26.9R - 5.725)]^{0.25}$
  - $n = 5.95$
  - $S = 26.9R - 5.725$
  - $C_0 = 1.02 \times 10^{-12} S$
- $\Delta K_I \geq 17.74[(3.75R + 0.06)/(26.9R - 5.725)]^{0.25}$
  - $n = 1.95$
  - $S = 3.75R + 0.06$
  - $C_0 = 1.01 \times 10^{-7} S$

$0.65 \leq R \leq 1.00$
- $\Delta K_I < 12.04$
  - $n = 5.95$
  - $S = 11.76$
  - $C_0 = 1.02 \times 10^{-12} S$
- $\Delta K_I \geq 12.04$
  - $n = 1.95$
  - $S = 2.5$
  - $C_0 = 1.01 \times 10^{-7} S$

Additionally, per A-4300(b)(2) of *ASME Section XI* (Reference 4), if the fatigue crack growth rate from light-water reactor environments is lower than air environments, then the rate in air should be used. Per A-4300(b)(1), the fatigue crack growth constants for flaws in an air environment are:

$n = 3.07$
$C_o = 1.99 \times 10^{-10} S$

S is a scaling parameter to account for the R ratio and is given by

$$S = 25.72\ (2.88 - R)^{-3.07}$$

Where $0 \leq R \leq 1$ and $\Delta K_I = K_{max} - K_{min}$.

For $R < 0$, ΔK_I depends on the crack depth, a, and the flow stress, σ_f. The flow stress is defined by (σ_{ys} is the yield strength and σ_{ult} is the ultimate tensile strength):

$$\sigma_f = \tfrac{1}{2}(\sigma_{ys} + \sigma_{ult})$$

For $-2 \leq R \leq 0$ and $K_{max} - K_{min} \leq (0.8)\times 1.12\sigma_f\sqrt{\pi a}$

$$S = 1$$
$$\Delta K_I = K_{max}.$$

For $R < -2$ and $K_{max} - K_{min} \leq (0.8)\times 1.12\sigma_f\sqrt{\pi a}$

$$S = 1$$
$$\Delta K_I = (1 - R)\ K_{max}/3.$$

For $R < 0$ and $K_{max} - K_{min} > (0.8)\times 1.12\sigma_f\sqrt{\pi a}$,

$$S = 1$$
$$\Delta K_I = K_{max} - K_{min}.$$

Where the *(0.8)* reduction factor is established by *NRC 10 CFR 50.55a*, item (xxviii), Section XI condition: Analysis of Flaws (Reference 11).

2.3.2 Stress Corrosion Crack Growth

Reference 12 conducted a stress corrosion cracking (SCC) susceptibility assessment that is specifically applicable to the Peach Bottom Unit 2 N16-A Reactor Vessel Nozzle. This calculation performs an extensive review of BWR operating experience to determine if low alloy steel is susceptible to stress corrosion cracking (SCC). In most cases of through-cladding SCC cracks in BWR reactor vessels, [ ]

The corrosion evaluation (Reference 12) concludes that extensive operating experience indicates that SCC of the exposed low alloy steel is [ ] However, this evaluation conservatively uses a constant SCC growth rate of [ ] based on the work presented in [ ] Section 3.4 of Reference 12 presents justification for use of this rate for constant loading conditions above [ ]

2.4 Flaw Evaluation Acceptance Criteria

The screening criteria provided in *ASME Code Case N-749* (Reference 5), as modified by the *NRC Federal Register, Volume 81, Page 10787 (81 FR 10787)* (Reference 6), as detailed in Section 2.4.1, is used to determine the appropriate method of analysis: linear elastic fracture mechanics (LEFM) or elastic-plastic fracture mechanics (EPFM). For LEFM flaw evaluations, the stress intensity factors are compared to the available fracture toughness values as detailed in Section 2.4.2, with appropriate safety factors applied per Table 2-1. When the material is more ductile and EPFM is the appropriate analysis method, the flaw evaluation is done in accordance with ASME Code Case N-749 (Reference 4), as detailed in Section 2.4.3, with appropriate safety factors applied per Table 2-1.

Table 2-1: Safety Factors for Flaw Acceptance

LEFM(1)			
Operating Condition	**Evaluation Method**	**Fracture Toughness / K_I**	
Normal/Upset	K_{IC} fracture toughness	$\sqrt{10} = 3.16$ or $\sqrt{2} = 1.41$ (1a, 1b)	
Emergency/Faulted	K_{IC} fracture toughness	$\sqrt{2} = 1.41$ (1c)	
EPFM Based on Limited Ductile Flaw Extension(2)			
Operating Condition	**Evaluation Method**	**Primary**	**Secondary**
Normal/Upset	$J_{0.1}$ limited flaw extension	2.0	1.0
Emergency/Faulted	$J_{0.1}$ limited flaw extension	1.5	1.0
EPFM Based on Limited Ductile Flaw Extension and Stability(3)			
Operating Condition	**Evaluation Method**	**Primary**	**Secondary**
Normal/Upset	*J/T* based flaw stability	2.14	1.0
Normal/Upset	$J_{0.1}$ limited flaw extension	1.5	1.0
Emergency/Faulted	*J/T* based flaw stability	1.2	1.0
Emergency/Faulted	$J_{0.1}$ limited flaw extension	1.25	1.0

Note(s):

(1) LEFM safety factors are from IWB-3613 of ASME Section XI (Reference 4).
  a. Per IWB-3613(a), for conditions where pressurization does not exceed 20% of the design pressure during which the minimum temperature is not less than RT_{NDT}:
     $K_I < K_{Ic}/\sqrt{2}$
  b. Per IWB-3613(b), for Normal and Upset conditions excluding those described in IWB-3613(a):
     $K_I < K_{Ic}/\sqrt{10}$ (criteria of IWB-3612(a))
  c. Per IWB-3613(c), for Emergency and Faulted conditions:
     $K_I < K_{Ic}/\sqrt{2}$ (criteria of IWB-3612(b))

(2) EPFM safety factors are based on Section 3.1 of Code Case N-749 (Reference 5).

(3) EPFM safety factors are based on Section 3.2 of Code Case N-749 (Reference 5).

2.4.1 Screening Criteria

ASME Code Case N-749 (Reference 5), states that EPFM acceptance criteria are applicable to ferritic steel components on the upper shelf of the Charpy energy curve when the metal temperature exceeds the upper shelf transition temperature, T_c. The NRC has proposed a modification to the Code Case definition of T_c, which is given below.

$$T_c = 154.8°F + 0.82 \times RT_{NDT} \text{ (U.S. Customary Units)}$$

Where RT_{NDT} is the adjusted reference nil-ductility temperature. When the metal temperature exceeds T_c, EPFM analysis is applicable.

Additionally, per Revision 19 of RG 1.147 (Reference 14), a temperature below T_{c1} requires the LEFM method to be applied:

$$T_{c1} = 95.36°F + 0.703 \times RT_{NDT} \text{ (U.S. Customary Units)}$$

Per RG 1.147 (Reference 14), between T_{c1} and T_c, while the fracture mode is in transition from LEFM to EPFM, users should consider whether it is appropriate to apply the EPFM method.

2.4.2 Linear Elastic Fracture Mechanics

LEFM is used to assess the potential for non-ductile failure. After the crack growth is calculated, the flaw is evaluated using Linear Elastic Fracture Mechanics (LEFM) methods. Article IWB-3612 of *Section XI* (Reference 4) requires that the applied stress intensity factor be less than the available fracture toughness at the crack tip temperature, with appropriate safety factor, as outlined below (Table 2-1).

IWB-3613(a): For conditions where pressurization does not exceed 20% of the design pressure during which the minimum temperature is not less than RT_{NDT}:

$K_I < K_{Ic} /\sqrt{2}$

IWB-3613(b): For Normal and Upset conditions excluding those described in IWB-3613(a):

$K_I < K_{Ic} /\sqrt{10}$ (criteria of IWB-3612(a))

IWB-3613(c): For Emergency and Faulted conditions:

$K_I < K_{Ic} /\sqrt{2}$ (criteria of IWB-3612(b))

In the above, K_{Ic} is the fracture toughness based on crack initiation for the corresponding crack-tip temperature. In the evaluation of the above limits, a plastic zone correction is incorporated using the methodology described in Section 2.2.2.

2.4.3 Elastic-Plastic Fracture Mechanics

EPFM is used as an alternative acceptance criteria when the flaw related failure mechanism is unstable ductile tearing. Elastic-plastic fracture mechanics analysis is performed based on *ASME Code Case N-749* (Reference 5) to evaluate crack driving force and flaw stability (if applicable). Two possible sets of acceptance criteria for EPFM are defined in *Code Case N-749* (Reference 5):

- Section 3.1 Acceptance Criteria Based Solely on Limited Ductile Crack Extension, or
- Section 3.2 Acceptance Criteria Based on Limited Ductile Crack Extension and Stability.

Section 3.1 of *N-749* (Reference 5) states that the flaw is acceptable if the crack driving force, as measured by the applied J-integral (J_{app}) with appropriate safety factors applied to the loads, is less than the J-integral of the material (J_{mat}) at a ductile crack extension of 0.1 inch ($J_{0.1}$). If the criteria of Section 3.1 of Reference 5 are not met, the flaw may still be acceptable if the criteria of Section 3.2 of Reference 5 are met. Section 3.2 allows lower safety factors for the crack driving force check, and additionally requires that flaw stability be evaluated with appropriate safety factors.

The flaw stability analysis is performed using a J-integral/tearing modulus (J-T) diagram to evaluate flaw stability under ductile tearing, where J is either the applied (J_{app}) or the material (J_{mat}) J-integral, and T is the tearing modulus, defined as $(E/\sigma_f^2)(\partial J/\partial a)$. Flaw stability and crack driving force assessments utilize the safety factors from Code Case N-749 (Reference 5) as outlined in Table 2-1.

The general methodology for performing EPFM analyses is outlined below.

E’	$= E/(1-\nu^2)$
Final flaw depth	$= a$
Total applied $K_I^{(1)}$	$= K_{Iapp}$
K_I due to residual stresses (secondary)	$= K_{Iwrs}$
K_I due to residual plus pressure	$= K_{Ip+wrs}$
K_I due to pressure (primary)	$= K_{Ip} = K_{Ip+wrs} - K_{Iwrs}$
K_I due to residual + thermal loads (secondary)$^{(1)}$	$= K_{Is} = K_{Iapp} - K_{Ip}$
Safety factor on primary loads	$= SF_p$
Safety factor on secondary loads	$= SF_s$

Total applied K_I with safety factors, K_I* $= SF_p \ x \ K_{Ip} + SF_s \ x \ K_{Is}$

Note (1): The total applied K_{Iapp} and the secondary K_{Is} conservatively include the effect of weld residual stresses.

For small scale yielding at the crack tip, a plastic zone correction (see Section 2.2.2) is used to calculate an effective flaw depth based on:

$$a_e = a + \frac{1}{6\pi}\left(\frac{K_I^*}{\sigma_y}\right)^2$$

The above equation is used to update the total applied stress intensity factor based on the following equation:

$$K_I' = K_I^*\sqrt{\frac{a_e}{a}}$$

The applied J-integral is then calculated using the following relationship:

$$J_{app} = \frac{(K_I^*)^2}{E'}$$

The applied J-integral is checked against $J_{0.1}$, demonstrating that the crack driving force falls below the J-R curve at a crack extension of 0.1 inch.

For flaw stability analysis, the final parameter needed to construct the J-T diagram is the tearing modulus. The applied tearing modulus, T_{app}, is calculated by numerical differentiation for small increments of crack size (da) about the crack size (a), according to:

$$T_{app} = \frac{E}{\sigma_f^2}\left(\frac{J_{app}(a+da) - J_{app}(a-da)}{2da}\right)$$

The material J-T curve is determined as described in Section 0 by constructing the J-T diagram as shown in Figure 2-1.

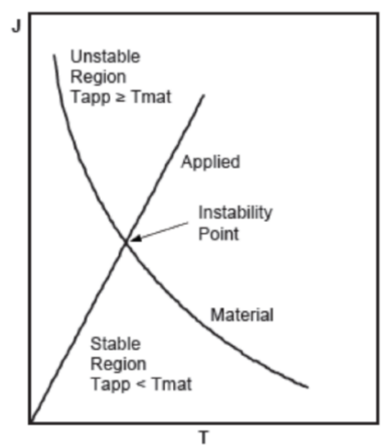

Figure 2-1: J-T Diagram

Flaw stability is demonstrated at an applied J-integral when the applied tearing modulus is less than the material tearing modulus. Alternately, the applied J-integral is less than the J-integral at the point of instability.

2.5 Primary Stress: Limit Load Analysis and Acceptance Criteria

The Limit load analysis is used to check for plastic collapse and is performed to demonstrate that Items 3.1(c) or 3.2(a)(3) of *N-749* are satisfied. Items 3.1(c) and 3.2(a)(3) of *N-749* (Reference 5) state that the flawed component must meet the primary stress limits of NB-3000 (Reference 15), assuming a local area reduction of the pressure retaining membrane that is equal to the area of the flaw. To evaluate the requirement, article NB-3228.1 of *Section III of the ASME Code* (Reference 15) is utilized. NB-3228.1 states that the limits on General Membrane Stress Intensity (NB-3221.1), Local Membrane Stress Intensity (NB-3221.2), and Primary Membrane plus Primary Bending Stress Intensity (NB-3221.3) need not be satisfied at a specific location if it can be shown by limit analysis that the specified loadings do not exceed two-thirds of the lower bound collapse load. The yield strength of the material to be used in these calculations is $1.5S_m$. Per NB-3112.1(a), the Design Pressure shall be used in showing compliance with this limit.

3.0 ASSUMPTIONS

3.1 Unverified Assumption

No unverified assumptions are used in this calculation.

3.2 Justified Assumptions and Modeling Simplifications

The following justified assumptions and modeling simplifications are used:

[ ]

4.0 DESIGN INPUTS

4.1 Geometry

The N16A instrument nozzle geometry for the original and repair configurations are obtained from References 20, 21, 22 and 23, with key dimensions listed in Table 4-1. Figure 4-1 shows the final repair configuration.

Table 4-1: Key Dimensions

Dimension	Equation	Value	Unit	Reference
Radius to Base Metal	R_s		in	
Reactor Vessel Wall Thickness (min)	t_s		in	
Cladding Thickness (nominal)	t_c		in	
Inside Diameter of Original Nozzle	ID_{ON}		in	
Outside Diameter of Original Nozzle	OD_{ON}		in	
Depth of Original JGW (from cladding)	H_{JGW}		in	
Diameter of Bore at J-Groove Weld	D_B		in	
As-Built Weld Pad Thickness (average, M2)	t_{WP}		in	
As-Built Overbore Diameter (close to bottom)	D_{OB}		in	
As-Built Overbore Depth (M8)	H_{OB}		in	
Inside Diameter of Replacement Nozzle (Small)	ID_{NNS}		in	
Inside Diameter of Replacement Nozzle (Large)	ID_{NNL}		in	
Outside Diameter of Replacement Nozzle	OD_{NN}		in	
NJGW Width/Depth into WP	W_{NJGW}		in	

Note(s):

(1) [

]

[ ]

Figure 4-1: Geometry – Final Repair Configuration

4.2 Material

Table 4-2 provides the material designations of the components.

Table 4-2: Component Material Designation

Component	Material Designation	Material Properties	Reference
RV Shell	SA-302 Gr. B modified by Code Case 1339	Table 4-3	3
Cladding	[		
Original JGW			
Original Nozzle			
Replacement Nozzle			
Weld Pad and NJGW			]

Note(s):

(1) [ ]

4.2.1 Mechanical Properties

Temperature (T) dependent material properties for the component materials specified in Table 4-2 are obtained from the ASME B&PV Code, Section II, 2013 Edition (Reference 24) per Reference 3. The Young's Modulus (E), Poisson's Ratio (ν), Density (ρ), Coefficient of Thermal Expansion (α), Thermal Conductivity (k), Specific Heat (C), Design Stress Intensity (S_m), Yield Strength (S_y) and Ultimate Strength (S_y) values are listed in Table 4-3 though Table 4-6. The material properties for the operating stress analysis (described in Section 2.1) are defined in [ ]

Table 4-3: [ ] Material Properties

T	E	ν	ρ	α	k	C	S_m	S_y	S_u
°F	psi	n/a	lb/in^3	in/in/°F	Btu/hr·in·°F	Btu/lb·°F	ksi	ksi	ksi

[ ]

Table 4-4: [ ] Material Properties

T	E	ν	ρ	α	k	C	S_m	S_y	S_u
°F	psi	n/a	lb/in^3	in/in/°F	Btu/hr·in·°F	Btu/lb·°F	ksi	ksi	ksi

[ ]

Table 4-5: [ ] Material Properties

T	E	ν	ρ	α	k	C
°F	psi	n/a	lb/in³	in/in/°F	Btu/hr·in·°F	Btu/lb·°F

[ ]

Table 4-6: [ ] Material Properties

T	E	ν	ρ	α	k	C
°F	psi	n/a	lb/in³	in/in/°F	Btu/hr·in·°F	Btu/lb·°F

[ ]

4.2.2 Fracture Material Properties

Per Reference [ ] the [ ] adjusted reference nil-ductility temperature RT_{NDT} (ART) of the N16 water level instrumentation nozzle [ ] This value of RT_{NDT} is utilized with the K_{Ic} fracture toughness for crack initiation curve defined in Article A-4200 of Section XI (Reference 4) as:

$$K_{Ic} = 33.2 + 20.734 \exp\left[0.02(T - RT_{NDT})\right]$$

Where T is the crack tip temperature, K_{Ic} is in units of $ksi\sqrt{in}$, and T and RT_{NDT} are in units of °F. In the present calculations, K_{Ic} is limited to a maximum value of [ ] The crack initiation K_{Ic} upper shelf toughness of [ ] is achieved at $T\text{-}RT_{NDT}$ > [ ]

The *J*-integral resistance (*J-R*) curve, needed for the EPFM method of analysis, is obtained from the following correlation for reactor pressure vessel plate in Regulatory Guide 1.161, Section 3.3.1 (Reference 2):

$$J_{mat} = MF\{C_1(\Delta a)^{C_2} exp(C_3(\Delta a)^{C_4})\}$$

Where MF is a margin factor, and Δa is the crack extension. C_1, C_2, C_3, and C_4 are coefficients which depend on the crack tip temperature and the Charpy V-notch upper-shelf energy as defined below:

$$C_1 = \exp(-2.44 + 1.13\ ln(CVN) - 0.00277T)$$
$$C_2 = 0.077 + 0.116\ lnC_1$$
$$C_3 = -0.0812 - 0.0092\ lnC_1$$
$$C_4 = -0.409$$

Where CVN is the Charpy V-notch upper-shelf energy in ft-lbs, and T is the crack tip temperature in °F. The margin factor, MF, of [ ] is utilized for the analysis for all cases, which provides a conservative *J-R* curve as
required by Reference 5. Section 3.3.1 of Reference 2 states that the use of this model should be justified if the sulfur content of the plate is greater than *0.018 wt.%*. Per Reference 25, the nozzle 16A is located in a section [ ] Per Reference 26, [ ] and, therefore, the use of this model is applicable.

Reference 21 states that an equivalent margin analysis (EMA) was performed at [ ] and approved by the NRC, which confirms that the Charpy V-notch upper-shelf energy (*CVN*) is greater than [ ] In addition, Reference 27 states that [ ] values for percent decrease in USE remain below the [ ] limits. Therefore, a *CVN* of [ ] is used in both the longitudinal and transverse directions. The resulting material J-R curve are plotted in Figure 4-2 for several temperatures for a USE of [ ]

[ ]

Figure 4-2: J-R Curves as a Function of Temperature, USE [ ]

The material tearing modulus is calculated using the following equation:

$$T_{mat} = \left(\frac{E}{\sigma_f^2}\right)\frac{\partial J_{mat}}{\partial a}$$

Where E is the Elastic Modulus, σ_f is the flow stress defined as $0.5(\sigma_y + \sigma_u)$, and the derivative of the *J-R* curve is:

$$\frac{\partial J_{mat}}{\partial a} = MF\{C_1C_2(\Delta a)^{C_2-1} + C_1C_3C_4(\Delta a)^{C_2+C_4-1}\}exp(C_3(\Delta a)^{C_4})$$

4.3 Design and Steady State Operating Conditions

Design and steady state operating conditions are listed in Table 4-7.

Table 4-7: Design and Steady State Operating Conditions

Parameter	Value	Unit	Reference
Design Temperature	[	°F	[
Design Pressure		psig	
Steady State Operating Temperature		°F	
Steady State Operating Pressure	]	psig	]

4.4 Operating Condition Transients

Table 4-8 lists the operating transients considered for this analysis, which are the transients deemed significant for flaw growth evaluations identified in Section 4.3.1 and A.4.2 of Reference 1. In addition, the [ ] transient is considered. Projected 80 year cycles for these transients are obtained from Reference [ ] Pro-rated cycles are then calculated for 34 years by ratioing the projected 80 year cycles by 34/80, since flaw growth is calculated starting from the time of nozzle repair in 2020 through the end of 80 year operation in 2054. Detailed pressure and thermal time history for the applicable transients are listed in Table 4-9 through Table 4-13. The source for the [ ] transients are described in Section [ ] with the time history temperature and pressure data obtained from Reference [ ] Per Section [ ] is applicable for this analysis, [ ] In addition, the heat transfer coefficient values used in the thermal transient analyses are listed in Table 4-14.

Table 4-8: Bounding Transients

Transient Name	Transient Abbreviation	Condition	Pressure/ Temperature Conditions	Projected 80 Year Cycles	Pro-Rated 34 Year Cycles(3)

Table 4-9: [ ] Transient

Time (s)	Temperature (°F)	Pressure (psig)

Table 4-10: [ ] Transient

Time (s)	Temperature (°F)	Pressure (psig)

[ ]

Table 4-11: [ ] Transient

Time (s)	Temperature (°F)	Pressure (psig)

[ ]

Table 4-12: [ ] Transient

Time (s)	Temperature (°F)	Pressure (psig)

[ ]

Table 4-13: [ ] Transient

Time (s)	Temperature (°F)	Pressure (psig)

[ ]

Table 4-14: Heat Transfer Coefficients

Location	Heat Transfer Coefficient (HTC)		Reference
	(BTU/hr-ft^2-°F)	(BTU/s-in^2-°F)$^{(1)}$	

[ ]

5.0 COMPUTER USAGE

5.1 Hardware / Software

ANSYS Release 19.2 (latest EASI list version), Reference 29, is used for all FEA runs documented herein. Use of this version of ANSYS is acceptable since there are no error notices applicable to this analysis.

Results of the calculations confirm that the inputs and structural responses of the models developed are within the range of applicability of ANSYS Mechanical Enterprise for these types of physical problems.

Computer runs are performed under controlled access of ANSYS Mechanical Enterprise, 19.2 on the approved platform 'Lynchburg HPCv2'. The computer used for this analysis is a multi-node server (auslynchpcc07), the computing nodes used to run this analysis were selected automatically by queuing handling software to be 'auslynchpc60'.

The hardware platform for node 'auslynchpc60': Intel® Xeon® 6136 CPU @ 3.00GHz, 262 GB; operating system: Red Hat Enterprise Server release 6.4 (Santiago); kernel:2.6.32-696.28.1.el6.x86_64.

5.2 Computer Files

Table 5-1 lists the computer files and location in the ColdStor directory.

Table 5-1: Computer Files

[/][cold]/[General-Access]/[32]/[32-9000000]/[32-9335342-000]/[official]/[00_OSA]/[ThermalAnalysis]/

Name	Size	Date/Time Modified	CRC
	55639	Oct 04 2021 10:40:51	15934
	55200	Oct 04 2021 10:40:54	59102
	38864	Oct 04 2021 10:40:57	04175
	35773	Oct 04 2021 10:40:59	09326
ThermalTransients.inp	13307	Sep 20 2021 10:50:28	57005
ThermalTransients.out	829529	Oct 04 2021 10:40:48	47870
dTpostProcessing.mac	4998	Sep 07 2021 16:02:51	08574

[/][cold]/[General-Access]/[32]/[32-9000000]/[32-9335342-000]/[official]/[00_OSA]/[StructuralAnalysis]/

Name	Size	Date/Time Modified	CRC
	326	Dec 03 2021 14:59:12	32702
	36428	Dec 06 2021 20:43:06	48338
	310	Sep 11 2021 09:24:31	30981
	223742	Oct 04 2021 11:29:18	55036
	316	Sep 11 2021 09:24:48	04021
	244014	Oct 04 2021 12:21:54	63647
	323	Sep 11 2021 09:36:19	42197
	99585	Oct 04 2021 12:38:10	41186
	314	Sep 11 2021 09:36:08	49425
	74815	Oct 04 2021 12:48:13	35276
	3155	Dec 06 2021 12:56:00	55383
	14987	Sep 20 2021 13:36:44	63601

[/][cold]/[General-Access]/[32]/[32-9000000]/[32-9335342-000]/[official]/[00_OSA]/[PostProcessing]/

Name	Size	Date/Time Modified	CRC
	1161544	Dec 06 2021 20:43:15	32143
	4345041	Oct 04 2021 12:48:46	16888
	14185126	Dec 06 2021 02:40:57	13229
	594528	Oct 04 2021 12:50:39	07177
	4631	Dec 06 2021 02:15:24	47301
	4793	Dec 06 2021 02:14:58	31595
	139026	Dec 06 2021 20:43:15	32963
	294	Sep 09 2021 18:05:07	22640
	546367	Oct 04 2021 12:48:46	56756
	299	Sep 20 2021 13:37:57	53953
	1823134	Dec 06 2021 02:40:57	35839
	246	Sep 08 2021 11:44:27	51677
	58538	Oct 04 2021 12:50:40	40645
	293	Sep 09 2021 18:05:25	56310
	584046	Dec 06 2021 02:41:34	55951
	292	Sep 09 2021 18:04:20	06894
	358758	Dec 06 2021 02:41:57	55943
	247	Sep 08 2021 11:44:57	56365
	58325	Oct 04 2021 12:51:41	17894
	4634500	Dec 06 2021 02:41:34	22746
	2898022	Dec 06 2021 02:41:57	49730
	594553	Oct 04 2021 12:51:40	40485

[/][cold]/[General-Access]/[32]/[32-9000000]/[32-9335342-000]/[official]/[01_Model]/

Name	Size	Date/Time Modified	CRC
Base_model.inp	24742780	Sep 28 2021 12:30:54	63258
CrackFanMesh2.mac	6655	Mar 09 2017 09:15:21	44896
gen_crack_models.inp	11765	Sep 28 2021 12:31:20	62832
gen_crack_models.out	1138610	Oct 04 2021 12:53:39	48977
hoop1a_merge.out	887243	Oct 04 2021 12:52:10	53054
hoop2a_merge.out	887915	Oct 04 2021 12:52:39	34427
hoop3a_merge.out	887915	Oct 04 2021 12:53:08	35723
hoop4a_merge.out	887915	Oct 04 2021 12:53:37	27299
materials.inp	7790	Sep 27 2021 13:37:52	11294

[/][cold]/[General-Access]/[32]/[32-9000000]/[32-9335342-000]/[official]/[02_KI_Transient]/

Name	Size	Date/Time Modified	CRC
	2781	Dec 06 2021 21:05:50	40714
	2781	Dec 06 2021 21:41:10	15272
	2781	Dec 06 2021 22:33:58	56399
	2781	Dec 06 2021 23:48:51	15683
	5206	Oct 11 2017 11:47:16	05783
	5773	Oct 04 2021 14:29:04	26724

	5773	Oct 05 2021 01:14:24	65049
	5773	Oct 05 2021 18:02:13	59409
	5773	Oct 06 2021 19:04:52	51890
	15021	Dec 06 2021 08:03:09	03590
	15021	Dec 06 2021 16:15:04	19831
	15021	Dec 07 2021 04:52:17	10576
	15021	Dec 07 2021 22:59:10	55064
	6045	Dec 07 2021 00:13:33	29789
	6045	Dec 07 2021 02:51:26	13875
	6045	Dec 07 2021 06:53:15	41935
	6045	Dec 07 2021 12:38:42	01498
	3747	Sep 28 2021 13:22:11	41983
	3752	Dec 03 2021 15:39:34	16161
	3742	Dec 06 2021 02:42:18	08296
	3742	Dec 06 2021 02:54:31	09576
	3742	Dec 06 2021 03:04:15	10854
	510	Dec 05 2017 12:38:34	54740
	31569499	Oct 07 2021 23:01:17	36391
	530	Dec 03 2021 15:25:13	14152
	1483873	Dec 06 2021 23:48:53	24714
	530	Dec 06 2021 02:46:59	05976
	17376217	Dec 07 2021 22:59:11	61870
	530	Dec 06 2021 02:53:01	02577
	5720993	Dec 07 2021 12:38:43	25677
	530	Dec 06 2021 03:03:39	61091
	3603655	Dec 06 2021 11:53:06	48335
	4413	Dec 06 2021 04:13:16	44933
	4413	Dec 06 2021 05:54:21	28019
	4413	Dec 06 2021 08:23:44	01895
	4413	Dec 06 2021 11:53:05	07192
	11570	Sep 28 2021 14:02:42	59459
	12392	Dec 06 2021 20:12:31	37192
	844	Oct 24 2017 08:24:29	52017

[/][cold]/[General-Access]/[32]/[32-9000000]/[32-9335342-000]/[official]/[03_KI_WRS]/

Name	Size	Date/Time Modified	CRC
Get_SIF.mac	5113	Oct 11 2017 12:41:41	61673
SIF_Driver_WRS.mac	3886	Oct 03 2021 22:10:23	35487
SIF_calc.inp	528	Dec 05 2017 12:45:03	03661
SIF_calc.out	728057	Oct 08 2021 00:02:14	65225
	2237	Oct 07 2021 23:08:42	23557
	2237	Oct 07 2021 23:20:09	47396
	2237	Oct 07 2021 23:37:35	46749
	2237	Oct 08 2021 00:02:14	20955

calc_k.mac	844	Oct 24 2017 08:24:29	52017

[/][cold]/[General-Access]/[32]/[32-9000000]/[32-9335342-000]/[official]/[04_KI_NO]/

Name	Size	Date/Time Modified	CRC
Get_SIF.mac	5117	Oct 11 2017 16:31:50	48377
[	2237	Oct 08 2021 00:09:33	53884
	2237	Oct 08 2021 00:21:15	07780
	2237	Oct 08 2021 00:38:50	49311
]	2237	Oct 08 2021 01:03:23	17289
SIF_Driver_NO.mac	3884	Oct 03 2021 22:11:09	53810
SIF_calc.inp	526	Dec 05 2017 12:46:03	26706
SIF_calc.out	722933	Oct 08 2021 01:03:24	35673
calc_k.mac	844	Oct 24 2017 08:24:29	52017

[/][cold]/[General-Access]/[32]/[32-9000000]/[32-9335342-000]/[official]/[05_LimitLoad]/

Name	Size	Date/Time Modified	CRC
Base_model_LL.inp	8219790	Sep 29 2021 16:06:54	06234
PB2_PRVS_LL.inp	2175	Sep 29 2021 16:10:41	22048
PB2_PRVS_LL.out	222014	Sep 29 2021 16:34:13	15829
materials_LL.inp	4278	Sep 29 2021 16:12:21	32517

[/][cold]/[General-Access]/[32]/[32-9000000]/[32-9335342-000]/[official]/[06_Spreadsheets]/

Name	Size	Date/Time Modified	CRC
EPFM-RG1161- [ ] .xlsm	198386	Dec 08 2021 01:06:26	03261
JR_RG_1161_ [ ] .xlsm	63609	Oct 07 2021 15:09:27	47000
LEFM_FCG.xlsm	674690	Dec 08 2021 01:06:36	17335

6.0 CALCULATIONS

6.1 Weld Residual plus Operating Stress Finite Element Analysis

As described in Section 2.1, for input into the finite element crack growth analysis detailed in Section 6.2, the combined residual plus operating transient stresses are calculated by utilizing the model developed in the WRS analysis (Reference 7). The final simulation provided in the WRS analysis is the welding of the new JGW (NJGW) to the new replacement nozzle and weld pad followed by [

] The final configuration from the Reference 7 WRS analysis, which is used for this analysis is shown in Figure 6-1.

The key operating transients are then applied to the model as follows, with the key operating transients defined in Section 4.4.

1. Thermal Analysis: A thermal transient analysis is performed for each applicable transient by [

   ]

2. Structural Analysis: A structural transient analysis is performed for each applicable transient by [

   ] The sequence of each applicable transient is defined as follows:

   a. [ ] of the [ ] are simulated at the end of the steady state operating cycles provided in Reference 7, followed by [ ] steady state operating condition [ ]

   b. [ ] for each remaining applicable transient is performed at the end of step 2.a above.

3. Post-Processing: The combined residual plus operating hoop stresses applicable for evaluating a postulated remnant flaw in the as-left J-groove weld are extracted [

   ]

See Section 3.2, Item 1 for justified assumptions and modeling simplifications used.

[ ]

Figure 6-1: Operating Stress Analysis Finite Element Model (Reference 7)

6.1.1 Thermal Analysis

For the thermal analysis, the *'Thermal_NJGW.db'* file is resumed from Reference 7. Temperature values listed in Table 4-9 through Table 4-12 for the four transients analyzed per Section 4.4 are [ ] The thermal run is documented in computer output file *'ThermalTransients.out'* (see Table 5-1).

The time-points for structural runs are selected based on the [ ] The thermal gradient listing can be found in computer files *'*_dT.out'* (see Table 5-1), with a list of time-points selected for the structural runs. Figure 6-3 through Figure 6-10 show the nodal temperature and thermal gradient output for each transient.

Figure 6-2: Thermal Gradients

[ ]

Figure 6-3: [ ] Nodal Temperature

[ ]

Figure 6-4: [ ] Nodal Thermal Gradients

[

]

Figure 6-5: [ ] Nodal Temperature

[

]

Figure 6-6: [ ] Nodal Thermal Gradients

Figure 6-7: [ ] Nodal Temperature

Figure 6-8: [ ] Nodal Thermal Gradients

[ ]

Figure 6-9: [ ] Nodal Temperature

[ ]

Figure 6-10: [ ] Nodal Thermal Gradients

6.1.2 Structural Analysis

Pressure is applied [ ] The displacements are [ ] the end cap pressure is [ ] The body temperature corresponding to the time of the transient is applied [ ] The timepoints for the structural runs are listed in Table 6-1, based on the [ ] The structural runs are documented in computer files ‘*Stress_*.out*’ (see Table 5-1).

[ ] of the [ ] are simulated [ ] of steady state operating condition (‘*Stress_OC.**’ files obtained from Reference 7). After the last cycle of [ ] of steady state operating condition is also applied. [ ] for the remaining applicable transients is performed at the [ ] starting at the steady state condition.

Table 6-1: Structural Run Time Points

[ ]		[ ]		[ ]		[ ]		[ ]		[ ]	
No.	Time (s)	No.	Time (s)	No.	Time (s)	No.	Time (s)	No.	Time (s)	No.	Time (s)

6.1.3 Post-Processing Results

The stresses applicable for evaluating a postulated remnant flaw in the as-left J-groove weld are extracted [ ] The operating transient stresses are extracted for all the time points listed in Table 6-1, and are contained in files [ ] obtained from files *'PostProcessing*.out'* (See Table 5-1). In addition, weld residual stresses are extracted from the Reference 7 analysis at the final cold shutdown state, contained in file [ ] and steady state conditions in file [ ] (see Table 5-1). Table 6-2 summarizes the computer output files applicable for evaluation a postulated remnant flaw in the as-left JGW.

[ ]

Figure 6-11: Zero (0) Degree Nodes for Stress Extraction

[ ]

Figure 6-12: Ninety (90) Degree Nodes for Stress Extraction

Table 6-2: Weld Residual plus Operating Stress Results Computer Output Files

Loading Condition	Computer File (Table 5-1)

[ ]

6.2 Explicit Flaw Finite Element Analysis

As described in Section 2.2, a radial-axial flaw is postulated in the JGW to obtain stress intensity factors (SIF) for each loading condition at varying positions along the crack front. Radial is with respect to the nozzle axis extending from the inside corner of the penetration to the interface between the JGW and the reactor vessel shell. [ ] Detailed analysis steps are as follows:

1. Finite Element Models: Develop a [ ] finite element crack model [ ] with crack tip elements [ ] capable of representing [ ] flaw depths (Figure 6-13). The model includes the [ ] The initial flaw size, a_o, is characterized by the [ ] finite element models are then generated as depicted in Figure 6-15, with flaw size increments of [ ] These models are used to obtain SIFs at [ ] positions along the crack front for residual and operating stresses, with crack face pressure.
2. Applied Loads: A [ ] is developed to transfer stresses from the uncracked finite element stress analysis (provided in Table 6-2) to the crack face of the cracked models. [ ]
3. Stress Intensity Factors: Obtain stress intensity factors (SIF) for each loading condition at varying positions along the crack front by using the [ ] Details of the SIF solutions and plastic zone correction are provided in Sections 2.2.1 and 2.2.2.

6.2.1 Finite Element Model

The finite element model developed for this analysis is a [ ] model. The model is meshed using ANSYS element types [ ] The base geometry and mesh are generated in the input file *'Base_model.inp'* and the explicit crack models are then generated using the file *'gen_crack_models.inp'*. Figure 6-13 illustrates the base finite element model and mesh, the initial flaw size ([ ]) is illustrated in Figure 6-14, and the [ ] crack front models are illustrated in Figure 6-15. Mechanical material properties assigned to the model are per Section 4.2.1

Figure 6-13: Finite Element Model - Crack Growth Base Model

Figure 6-14: Finite Element Model – Initial Flaw Size

Figure 6-15: Finite Element Model - Crack Front Locations

6.2.2 Applied Loads

Stresses due to residual stresses and operating stresses, which are obtained from the [ ] stress analysis of the applicable operating transients described in Section 6.1 and summarized in Table 6-2, are applied to the explicit crack models. Stresses are [ ] to the crack face from the elastic plastic finite element stress model to the finite element crack model through [ ] The corresponding operating transient pressure is also applied to the crack face to account for the actual loading. Figure 6-16 shows an example of the weld residual stresses mapped onto Crack Face [ ]

[ ]

Figure 6-16: Weld Residual Stress Mapped to Crack Face [ ] (psi)

In addition to the [ ] stresses, the displacements are constrained normal to the face of the symmetry planes and the additional model cutting plane. The displacements of the nodes on the crack face are not constrained.

6.2.3 Stress Intensity Factors Results

SIFs are calculated for each postulated crack front using the stress results from the files listed in Table 6-2. The calculations are run by the ANSYS input file '*SIF_calc.inp*' (see Table 5-1). The ANSYS macro '*SIF_Driver.mac*' sets the crack face boundary conditions, [ ] Table 6-3 through Table 6-9 present the SIF results for use in Section 6.3.

Table 6-3: Stress Intensity Factors –WRS

Crack Front Position	K_I (psi√in) at Flaw Size (in)
1	
2	
3	
4	
5	
6	
7	
8	
9	
10	
11	
12	
13	
14	
15	
16	
17	
18	
19	
20	
21	
22	
23	
24	
25	
26	
27	
28	
29	

Table 6-4: Stress Intensity Factors – Steady State Normal Operating Condition

Crack Front Position	K_I (psi$\sqrt{in}$) at Flaw Size (in)
1	
2	
3	
4	
5	
6	
7	
8	
9	
10	
11	
12	
13	
14	
15	
16	
17	
18	
19	
20	
21	
22	
23	
24	
25	
26	
27	
28	
29	

Table 6-5: Stress Intensity Factors (SIF) – [ ]

Crack Front Position	Minimum K_I (psi√in) at Flaw Size (in)	Maximum K_I (psi√in) at Flaw Size (in)	[ ] - K_I (psi√in) at Flaw Size (in)
1	[		
2			
3			
4			
5			
6			
7			
8			
9			
10			
11			
12			
13			
14			
15			
16			
17			
18			
19			
20			
21			
22			
23			
24			
25			
26			
27			
28			
29			]

Table 6-6: Stress Intensity Factors (SIF) – [ ]

Crack Front Position	Minimum K_I (psi√in) at Flaw Size (in)	Maximum K_I (psi√in) at Flaw Size (in)
1		
2		
3		
4		
5		
6		
7		
8		
9		
10		
11		
12		
13		
14		
15		
16		
17		
18		
19		
20		
21		
22		
23		
24		
25		
26		
27		
28		
29		

Table 6-7: Stress Intensity Factors (SIF) – [ ]

Crack Front Position	Minimum K_I (psi√in) at Flaw Size (in)	Maximum K_I (psi√in) at Flaw Size (in)
1		
2		
3		
4		
5		
6		
7		
8		
9		
10		
11		
12		
13		
14		
15		
16		
17		
18		
19		
20		
21		
22		
23		
24		
25		
26		
27		
28		
29		

Table 6-8: Stress Intensity Factors (SIF) – [ ]

Crack Front Position	Minimum K_I (psi√in) at Flaw Size (in)	Maximum K_I (psi√in) at Flaw Size (in)	[ ] - K_I (psi√in) at Flaw Size (in)
1			
2			
3			
4			
5			
6			
7			
8			
9			
10			
11			
12			
13			
14			
15			
16			
17			
18			
19			
20			
21			
22			
23			
24			
25			
26			
27			
28			
29			

Table 6-9: Stress Intensity Factors (SIF) – [ ]

Crack Front Position	Minimum K_I (psi√in) at Flaw Size (in)	Maximum K_I (psi√in) at Flaw Size (in)
1		
2		
3		
4		
5		
6		
7		
8		
9		
10		
11		
12		
13		
14		
15		
16		
17		
18		
19		
20		
21		
22		
23		
24		
25		
26		
27		
28		
29		

[ ]

6.3 Flaw Growth Calculation

Utilizing the SIF solutions from Section 6.2, fatigue crack growth is calculated based on the fatigue crack growth rule identified in Section 2.3.1, integrated numerically as follows:

$$\frac{da}{dN} = \frac{\Delta a}{\Delta N} = C_0(\Delta K_I)^n \;\; or \;\; \Delta a = \Delta N C_0 (\Delta K_1)^n$$

The impact of the cycle increment (ΔN) is investigated, and it was found that [ ] Therefore, crack growth presented in this report has been calculated on a [ ] Crack growth is evaluated for 34 years of operation starting from the time of nozzle repair in 2020 through the end of 80 year operation in 2054.

The stress intensity factors at all positions are assessed, and it is determined that position [ ] is bounding since it produces the largest crack growth. Therefore, fatigue crack growth calculations for position [ ] are performed in the spreadsheet '*LEFM_FCG.xlsm*' (see Table 5-1), and the detailed results are shown in Table 6-10 through Table 6-12. Note that the [ ] transient is designated as an [ ]

Stress corrosion crack (SCC) growth is calculated in Table 6-14 using a constant crack growth rate as described in Section 2.3.2, with the steady state normal operating SIFs from Table 6-4.

The final flaw size includes fatigue crack growth from all applicable transients and SCC crack growth.

Table 6-10: Fatigue Crack Growth - [ ]

Transient Name =	[
Transient ID =	
Total Cycles =	
Design Life =	
Cycles/Year =	
Cycles/Week =	
Step Fluid Temperature (F) =	]

Operating Time	Cycles	a	$K_{Max}(a)$	$K_{Min}(a)$	ΔKI	Δa
Years		in	ksi√in	ksi√in	ksi√in	in
[						]

Operating Time	Cycles	a	$K_{Max}(a)$	$K_{Min}(a)$	ΔKI	Δa
Years		in	ksi√in	ksi√in	ksi√in	in

Table 6-11: Fatigue Crack Growth - [ ]

Transient Name =	[ ]
Transient ID =	
Total Cycles =	
Design Life =	
Cycles/Year =	
Cycles/Week =	
Step Fluid Temperature (F) =	

Operating Time	Cycles	a	$K_{Max}(a)$	$K_{Min}(a)$	ΔKI	Δa
Years		in	ksi√in	ksi√in	ksi√in	in
[ ]						

Operating Time	Cycles	a	$K_{Max}(a)$	$K_{Min}(a)$	ΔKI	Δa
Years		in	ksi√in	ksi√in	ksi√in	in

Table 6-12: Fatigue Crack Growth - [ ]

Transient Name =	[
Transient ID =	
Total Cycles =	
Design Life =	
Cycles/Year =	
Cycles/Week =	
Step Fluid Temperature (F) =	]

[

Operating Time	Cycles	a	$K_{Max}(a)$	$K_{Min}(a)$	ΔKI	Δa
Years		in	ksi√in	ksi√in	ksi√in	in

]

Operating Time	Cycles	a	$K_{Max}(a)$	$K_{Min}(a)$	ΔKI	Δa
Years		in	ksi√in	ksi√in	ksi√in	in

Table 6-13: Fatigue Crack Growth - [ ]

Transient Name =	
Transient ID =	
Total Cycles =	
Design Life =	
Cycles/Year =	
Cycles/Week =	
Step Fluid Temperature (F) =	

Operating Time	Cycles	a	$K_{Max}(a)$	$K_{Min}(a)$	ΔKI	Δa
Years		in	ksi√in	ksi√in	ksi√in	in

[ ]

Operating Time	Cycles	a	$K_{Max}(a)$	$K_{Min}(a)$	ΔKI	Δa
Years		in	ksi√in	ksi√in	ksi√in	in

Table 6-14: Stress Corrosion Crack Growth

Operating Time	a	$K_I(a)$ at SS	$K_I(a)$ at SS	da/dt	Δa
Years	in	ksi√in	MPa√m	m/s	in

Operating Time	a	$K_I(a)$ at SS	$K_I(a)$ at SS	da/dt	Δa
Years	in	ksi√in	MPa√m	m/s	in

6.4 Flaw Evaluations

6.4.1 LEFM Evaluation

The LEFM evaluation is performed for the final flaw size obtained from the crack growth calculation detailed in Section 6.3. The applied SIF is evaluated accounting for the plastic zone correction described in Section 2.2.2, and its acceptability is evaluated based on the rules outlined in Section 2.4.2. The results for the bounding crack tip position [ ] are shown in Table 6-15 for the bounding transient cases.

Based on Section 2.4.1 screening criteria, the [ ] fluid temperature falls below T_c and T_{c1}, and therefore evaluation by LEFM is applicable. In addition, the [ ] case temperature falls between T_c and T_{c1}, and therefore per Section 2.4.1 screening criteria, users should consider whether it is appropriate to apply the EPFM method. Therefore, the [ ] case is evaluated for both LEFM and EPFM acceptance criteria for completeness. [ ] The remaining transients limiting load step temperature is above Tc, and therefore evaluation of EPFM criteria is applicable.

Table 6-15 results demonstrate that the LEFM acceptance criteria are met for 34 years of crack growth for the [ ] As noted above, the [ ] transients, which do not meet LEFM criteria are to be evaluated based on EPFM criteria, as demonstrated in Section 6.4.2.

Table 6-15: LEFM Results – Bounding Crack Tip Position [ ]

RT_{NDT}(4)	[	°F
EPFM Required Above Temperature T_C(4)		°F
LEFM Required Below Temperature, T_{c1}(5)		°F
Upper Shelf Toughness		ksi√in
Initial Flaw Size, a_i		in
Final Flaw Size, a_f		in
Crack Growth, Δa	]	in
Loading(1)	[	
Service Level		
Fluid Temperature (°F)(2)		
Pressure (psi)		
S_y (ksi)		
K_{Ic} (ksi√in)		
K(a) (ksi√in)		
a_e (in)		
$K(a_e)$ (ksi√in)		
Margin = $K_{Ic}/K(a_e)$		
Required Margin		
Acceptable By LEFM		
Meets T_C Criterion, EPFM Required		
Meets T_{C1} Criterion, LEFM Required		]

Note(s):

(1) LEFM evaluation is reported for the limiting load step cases of each transient. Additionally, a case where the fluid temperature is less than T_C is also reported for the [ ] transients.

(2) The maximum transient fluid temperature is selected for each transient for the [ ] cases.

(3) Pressure at [ ] load step does not exceed 20% of the design pressure; therefore acceptance criterion from IWB-3613(a) of Section XI (Reference 4) applies.

(4) T_c = 154.8°F + 0.82 x RT_{NDT} (U.S. Customary Units), with RT_{NDT} of [ ] per Section 4.2.2.

(5) T_{c1} = 95.36°F + 0.703 × RT_{NDT} (U.S. Customary Units)

6.4.2 EPFM Evaluation

For the postulated crack, the EPFM evaluations are performed for the final flaw size in accordance with the methodology described in Section 2.4.3 using the spreadsheet '*EPFM-RG1161-* [ ] *.xlsm*' (see Table 5-1). As noted in Section 2.4.3, these evaluations conservatively include the weld residual stress, which is not required by Code Case N-749 (Reference 5). In addition, the K_I due to pressure (K_{IP}) is calculated based on the steady state normal operating condition results (Table 6-4). The steady state condition K_I is interpolated or extrapolated for the desired flaw size (see Section 2.2) and multiplied by the ratio of the transient pressure to the steady state normal operating pressure.

As discussed in Section 6.4.1, based on Section 2.4.1 screening criteria, the [ ] cases are evaluated using EPFM criteria. Table 6-16 provides the results of the EPFM evaluations for the final flaw size using a USE of [ ] (Section 0). Note that when the higher safety factors (SF) provided in Section 3.1 of Code Case N-749 (Reference 5) are used for the applied *J*-Integral criterion, the stability check is not required. However, it is included here for completeness.

For the postulated crack, as shown in Table 6-16, all cases meet the EPFM acceptance criteria for 34 years of crack growth. Details of the calculations are shown in Table 6-17 through Table 6-21 and J-T Diagrams are shown in Figure 6-17 through Figure 6-21.

Table 6-16: EPFM Results – Crack Tip Position [ ]

	Loading	[
	Service Level	
	Temperature (°F)	
	Pressure (psi)	
Applied J-Integral Check	**Primary Safety Factor**	
	Secondary Safety Factor	
	J_{app} (kips/in)	
	$J_{0.1}$ (kips/in)	
	Margin = $J_{0.1}/J_{app}$	
	Required Margins	
	Applied J-Integral Check Acceptable	
	Stability Check Required	
Stability Check	**Primary Safety Factor**	
	Secondary Safety Factor	
	T_{app}	
	$T_{instability}$	
	Margin = $T_{instability}/T_{app}$	
	Required Margins	
	Stability Check Acceptable	]

Table 6-17: EPFM Evaluation for [ ]

EPFM Equations:	J_{app} =	$[KI'(a_e)]^2/E'$
	T_{app} =	$(E/\sigma_f^2)*(dJ_{app}/da)$
Applied J-Integral Criterion:	J_{app} <	$J_{0.1}$
	$J_{0.1}$ =	J_{mat} at Δa = 0.1 in.

N-749 Section	**Safety Factors**		**KI^*_p**	**KI^*_s**	**$KI^*(a)$**	**a_e**	**$KI'(a_e)$**	**J_{app}**	**$J_{0.1}$**	**OK (Yes/No)**
	Primary	**Secondary**	**(ksi√in)**	**(ksi√in)**	**(ksi√in)**	**(in.)**	**(ksi√in)**	**(kips/in)**	**(kips/in)**	
[										]

Ductile Crack Growth Stability Criterion:	T_{app} <	T_{mat}
At instability:	T_{app} =	T_{mat}

Safety Factors		**KI^*_p**	**KI^*_s**	**$KI^*(a)$**	**a_e**	**$KI'(a_e)$**	**J_{app}**	**T_{app}**	**Stable (Yes/No)**
Primary	**Secondary**	**(ksi√in)**	**(ksi√in)**	**(ksi√in)**	**(in.)**	**(ksi√in)**	**(kips/in)**		
[									]

Iterate on safety factor until T_{app} = T_{mat} to determine $J_{instability}$:

Safety Factors		**KI^*_p**	**KI^*_s**	**$KI^*(a)$**	**a_e**	**$KI'(a_e)$**	**$J_{instability}$**	**T_{app}**	**T_{mat}**
Primary	**Secondary**	**(ksi√in)**	**(ksi√in)**	**(ksi√in)**	**(in.)**	**(ksi√in)**	**(kips/in)**		
[									]

[ ]

Figure 6-17: J-T Diagram for [ ] and USE = [ ]

Table 6-18: EPFM Evaluation for [ ]

EPFM Equations:	J_{app} =	$[KI'(a_e)]^2/E'$
	T_{app} =	$(E/\sigma_f^2)*(dJ_{app}/da)$
Applied J-Integral Criterion:	J_{app} <	$J_{0.1}$
	$J_{0.1}$ =	J_{mat} at Δa = 0.1 in.

N-749 Section	Safety Factors		KI^*_p	KI^*_s	KI*(a)	a_e	$KI'(a_e)$	J_{app}	$J_{0.1}$	OK (Yes/No)
	Primary	Secondary	(ksi√in)	(ksi√in)	(ksi√in)	(in.)	(ksi√in)	(kips/in)	(kips/in)	
[										]

Ductile Crack Growth Stability Criterion:	T_{app} <	T_{mat}
At instability:	T_{app} =	T_{mat}

Safety Factors		KI^*_p	KI^*_s	KI*(a)	a_e	$KI'(a_e)$	J_{app}	T_{app}	Stable (Yes/No)
Primary	Secondary	(ksi√in)	(ksi√in)	(ksi√in)	(in.)	(ksi√in)	(kips/in)		
[									]

Iterate on safety factor until T_{app} = T_{mat} to determine $J_{instability}$:

Safety Factors		KI^*_p	KI^*_s	KI*(a)	a_e	$KI'(a_e)$	$J_{instability}$	T_{app}	T_{mat}
Primary	Secondary	(ksi√in)	(ksi√in)	(ksi√in)	(in.)	(ksi√in)	(kips/in)		
[									]

[ ]

Figure 6-18: J-T Diagram for [ ] and USE = [ ]

Table 6-19: EPFM Evaluation for [ ]

EPFM Equations:	J_{app} =	$[KI'(a_e)]^2/E'$
	T_{app} =	$(E/\sigma_f^2)*(dJ_{app}/da)$
Applied J-Integral Criterion:	J_{app} <	$J_{0.1}$
	$J_{0.1}$ =	J_{mat} at Δa = 0.1 in.

N-749 Section	**Safety Factors**		**KI^*_p**	**KI^*_s**	**KI*(a)**	**a_e**	**$KI'(a_e)$**	**J_{app}**	**$J_{0.1}$**	**OK (Yes/No)**
	Primary	**Secondary**	**(ksi√in)**	**(ksi√in)**	**(ksi√in)**	**(in.)**	**(ksi√in)**	**(kips/in)**	**(kips/in)**	
[										]

Ductile Crack Growth Stability Criterion:	T_{app} <	T_{mat}
At instability:	T_{app} =	T_{mat}

Safety Factors		**KI^*_p**	**KI^*_s**	**KI*(a)**	**a_e**	**$KI'(a_e)$**	**J_{app}**	**T_{app}**	**Stable (Yes/No)**
Primary	**Secondary**	**(ksi√in)**	**(ksi√in)**	**(ksi√in)**	**(in.)**	**(ksi√in)**	**(kips/in)**		
[									]

Iterate on safety factor until T_{app} = T_{mat} to determine $J_{instability}$:

Safety Factors		**KI^*_p**	**KI^*_s**	**KI*(a)**	**a_e**	**$KI'(a_e)$**	**$J_{instability}$**	**T_{app}**	**T_{mat}**
Primary	**Secondary**	**(ksi√in)**	**(ksi√in)**	**(ksi√in)**	**(in.)**	**(ksi√in)**	**(kips/in)**		
[									]

[ ]

Figure 6-19: J-T Diagram for [ ] and USE = [ ]

Table 6-20: EPFM Evaluation for [ ]

EPFM Equations:	J_{app} =	$[KI'(a_e)]^2/E'$
	T_{app} =	$(E/\sigma_f^2)*(dJ_{app}/da)$
Applied J-Integral Criterion:	J_{app} <	$J_{0.1}$
	$J_{0.1}$ =	J_{mat} at Δa = 0.1 in.

N-749 Section	Safety Factors		KI^*_p	KI^*_s	KI*(a)	a_e	$KI'(a_e)$	J_{app}	$J_{0.1}$	OK (Yes/No)
	Primary	Secondary	(ksi√in)	(ksi√in)	(ksi√in)	(in.)	(ksi√in)	(kips/in)	(kips/in)	

Ductile Crack Growth Stability Criterion:	T_{app} <	T_{mat}
At instability:	T_{app} =	T_{mat}

	Safety Factors		KI^*_p	KI^*_s	KI*(a)	a_e	$KI'(a_e)$	J_{app}	T_{app}	Stable (Yes/No)
	Primary	Secondary	(ksi√in)	(ksi√in)	(ksi√in)	(in.)	(ksi√in)	(kips/in)		

Iterate on safety factor until T_{app} = T_{mat} to determine $J_{instability}$:

Safety Factors		KI^*_p	KI^*_s	KI*(a)	a_e	$KI'(a_e)$	$J_{instability}$	T_{app}	T_{mat}
Primary	Secondary	(ksi√in)	(ksi√in)	(ksi√in)	(in.)	(ksi√in)	(kips/in)		

[ ]

Figure 6-20: J-T Diagram for [ ] and USE = [ ]

Table 6-21: EPFM Evaluation for [ ]

EPFM Equations:	J_{app} =	$[KI'(a_e)]^2/E'$
	T_{app} =	$(E/\sigma_f^2)*(dJ_{app}/da)$
Applied J-Integral Criterion:	J_{app} <	$J_{0.1}$
	$J_{0.1}$ =	J_{mat} at Δa = 0.1 in.

N-749 Section	Safety Factors		KI^*_p	KI^*_s	KI*(a)	a_e	$KI'(a_e)$	J_{app}	$J_{0.1}$	OK (Yes/No)
	Primary	Secondary	(ksi√in)	(ksi√in)	(ksi√in)	(in.)	(ksi√in)	(kips/in)	(kips/in)	
[										]

Ductile Crack Growth Stability Criterion:	T_{app} <	T_{mat}
At instability:	T_{app} =	T_{mat}

Safety Factors		KI^*_p	KI^*_s	KI*(a)	a_e	$KI'(a_e)$	J_{app}	T_{app}	Stable (Yes/No)
Primary	Secondary	(ksi√in)	(ksi√in)	(ksi√in)	(in.)	(ksi√in)	(kips/in)		
[									]

Iterate on safety factor until T_{app} = T_{mat} to determine $J_{instability}$:

Safety Factors		KI^*_p	KI^*_s	KI*(a)	a_e	$KI'(a_e)$	$J_{instability}$	T_{app}	T_{mat}
Primary	Secondary	(ksi√in)	(ksi√in)	(ksi√in)	(in.)	(ksi√in)	(kips/in)		
[									]

[ ]

Figure 6-21: J-T Diagram for [ ] and USE = [ ]

Table 6-22: EPFM Evaluation for [ ]

EPFM Equations:	$J_{app} = [KI'(a_e)]^2/E'$
	$T_{app} = (E/\sigma_f^2)*(dJ_{app}/da)$
Applied J-Integral Criterion:	$J_{app} < J_{0.1}$
	$J_{0.1} = J_{mat}$ at $\Delta a = 0.1$ in.

N-749 Section	Safety Factors		KI^*_p	KI^*_s	$KI^*(a)$	a_e	$KI'(a_e)$	J_{app}	$J_{0.1}$	OK (Yes/No)
	Primary	Secondary	(ksi√in)	(ksi√in)	(ksi√in)	(in.)	(ksi√in)	(kips/in)	(kips/in)	
[										]

Ductile Crack Growth Stability Criterion:	$T_{app} < T_{mat}$
At instability:	$T_{app} = T_{mat}$

Safety Factors		KI^*_p	KI^*_s	$KI^*(a)$	a_e	$KI'(a_e)$	J_{app}	T_{app}	Stable (Yes/No)
Primary	Secondary	(ksi√in)	(ksi√in)	(ksi√in)	(in.)	(ksi√in)	(kips/in)		
[									]

Iterate on safety factor until $T_{app} = T_{mat}$ to determine $J_{instability}$:

Safety Factors		KI^*_p	KI^*_s	$KI^*(a)$	a_e	$KI'(a_e)$	$J_{instability}$	T_{app}	T_{mat}
Primary	Secondary	(ksi√in)	(ksi√in)	(ksi√in)	(in.)	(ksi√in)	(kips/in)		
[									]

[ ]

Figure 6-22: J-T Diagram for [ ] and USE = [ ]

6.5 Primary Stress Evaluation - Limit Load Analysis

The acceptance criterion of items 3.1(c) and 3.2(a)(3) of Reference 5 require that the primary stress limits of NB-3000 (Reference 15) are met assuming a local area reduction of the pressure retaining membrane that is equal to the area of the flaw. As discussed in Section 2.5, the primary stress limits for design conditions (NB-3221.1, NB-3221.2, and NB-3221.3) need not be satisfied if it can be shown by performing a limit analysis (NB-3228.1) that the applied loadings do not exceed two-thirds of the lower bound collapse load. This condition is equivalent to showing that the structure does not collapse at a pressure (P_{min}) equal to 150% of the Design Pressure. In terms of finite element results, plastic collapse of the structure is equivalent to numerical instability.

For the finite element model, the cladding, JGW, original nozzle, and portions of the RV shell are not included in the model in order to represent the material removed by the postulated J-Groove flaws and crack growth. The removed material represents a crack growth of [ ] from the initial postulated flaw, which is slightly [ ] than the final crack growth of [ ] (Table 6-15). The resulting model geometry with material removed is shown in Figure 6-23.

The material properties for the analysis are defined in the file '*materials_LL.inp*'. Note that the cladding and the JGW weld are excluded from the model since structural credit cannot be taken for the cladding and the JGW is postulated to be flawed. The properties are identical to those used in the explicit crack models with the exception that the material has been changed to be elastic-perfectly plastic. The value of yield strength (S_y) used is based on [ ] (Table 4-7), as calculated below:

[ ]

Pressure is applied to the ID surfaces of the vessel and replacement nozzle and to the original nozzle bore, incrementally increasing in each load step. Displacements normal to two planes of symmetry and the cut face in the model are constrained. Additionally, end cap pressures are added to the end surfaces of the replacement nozzle and the RV. The analysis is run using the input file '*PB2_PRVS_LL.inp*' with results output to "*PB2_PRVS_LL.out*". The analysis is run up to a pressure of [ ] which is equal to [ ] which exceeds the requirement of 150% of the Design Pressure. The equivalent stress at the last load step is shown in Figure 6-24.

[ ]

Figure 6-23: Limit Load Finite Element Model

[ ]

Figure 6-24: Limit Load Analysis: Equivalent Stresses at the Final Load Step (psi)

7.0 SUMMARY OF RESULTS

A fatigue and SCC crack growth and fracture mechanics evaluation of the postulated flaw in the as-left JGW performed based on a combination of linear elastic and elastic-plastic fracture mechanics demonstrates that the postulated flaw is shown to be acceptable for 34 years of operation (from the time of nozzle repair in 2020 to the end of 80 year operation in 2054) utilizing the safety factors in Table 2-1, and the applicable *J-R* Curves from Regulatory Guide 1.161 (Reference 2). Table 6-15 summarize the LEFM results, which demonstrate that the IWB-3612 (Reference 4) acceptance criteria is met for 34 years of crack growth for transient cases where LEFM criteria is applicable. Table 6-16 summarizes the EPFM results, which demonstrate that the Code Case N-749 (Reference 5) acceptance criteria is met for 34 years of crack growth for the transient cases where EPFM criteria is applicable.

In addition, the primary stress criteria of IWB-3610(d)(2) (Reference 4) and 3.1(c) and 3.2(a)(3) of Code Case N-749 (Reference 5) are satisfied since the limit analysis performed in Section 6.5 shows that the structure does not collapse at a pressure equal to 150% of the Design Pressure.

8.0 REFERENCES

References identified with an (*) are maintained within Exelon Records System and are not retrievable from Framatome Records Management. These are acceptable references per Framatome Administrative Procedure 0402-01, Attachment 7. See page 2 for Project Manager Approval of customer references.

1. Framatome Document 32-9321034-002, "Peach Bottom 2 N16A Instrument Nozzle Repair J-Groove One-Cycle Justification."
2. Regulatory Guide 1.161, "Evaluation of Reactor Pressure Vessels with Charpy Upper-Shelf Energy Less than 50 ft-lb", June 1995.
3. Framatome Document 08-9320930-003, "Peach Bottom Unit 2 N16A Instrumentation Nozzle Replacement – Design Specification."
4. ASME Boiler &Pressure Vessel Code, Section XI, "Rules for Inservice Inspection of Nuclear Power Plant Components" 2013 Edition
5. Cases of the ASME Boiler and Pressure Vessel Code, Case N-749, "Alternative Acceptance Criteria for Flaws in Ferritic Steel Components Operating in the Upper Shelf Temperature Range," Section XI, Division 1, March 2012.
6. Federal Register, Volume 81, Page 10787 (81 FR 10787), Wednesday March 2, 2016, Proposed Rules.
7. Framatome Document 32-9334548-000, "Peach Bottom Unit 2 RV Instrument Nozzle N16A Repair Weld Residual Stress Analysis."
8. Framatome Document 38-9328911-000, "Framatome Design Input Request Documentation, TODI-PEDM-N16A-13, Revision 0."
9. Framatome Document 38-2201960-001, "Framatome Design Input Request Documentation, TODI-PEDM-N16A-15, Revision 1."
10. Anderson, T. L, "Fracture Mechanics – Fundamentals and Applications", CRC Press, 1991.
11. Code of Federal Regulations, Title 10, Part 50.55a, "Domestic Licensing of Production and Utilization Facilities, Codes and Standards", Federal Register Vol. 80, p. 45843, Aug. 3, 2015.
12. Framatome Document 51-9320932-001"Corrosion Evaluation of the Peach Bottom Unit 2 N16-A Reactor Vessel Nozzle Modification"
13. * BWRVIP-60-A: BWR Vessel and Internals Project, Evaluation of Stress Corrosion Crack Growth in Low Alloy Steel Vessel Materials in the BWR Environment, EPRI, Palo Alto, CA: June 2003. EPRI Technical Report 1008871.
14. U.S. NRC Regulatory Guide 1.147, Revision 19, "Inservice Inspection Code Case Acceptability, ASME Section XI, Division I", October 2019.
15. ASME Boiler and Pressure Vessel Code, Section III, "Rules for Construction of Nuclear Facility Components", Division 1, 2013.
16. ASME Boiler and Pressure Vessel Code, Section III, 1965 with Addenda to Winter 1965.
17. Framatome Document 32-2500012-002, "Materials Database for Weld Residual Stress Finite Element Analyses."
18. Materials Reliability Program: Welding Residual Stress Dissimilar Metal Butt-Weld Finite Element Modeling Handbook (MRP-317, Revision 1). EPRI, Palo Alto, CA: 2015. 3002005499.
19. Framatome Condition Report CR-2020-2586.
20. Framatome Drawing 02-8124069E-002, "Peach Bottom Unit 2 N16A Nozzle Replacement Implementation."
21. Framatome Document 38-2201949-000, "1st Transmittal of Design Information – Peach Bottom Unit 2, TODI-PEDM-N16A-1, Revision 0.
22. Framatome Document 50-9320938-000, "Completed Traveler – Peach Bottom 2, N16A Nozzle Repair During P2R23."
23. Framatome Drawing 02-9180866C-003, "2 Inch Instrumentation Replacement Nozzle."

24. ASME B&PV Code, Section II, Materials, ASME Code, 2013 Edition.
25. Framatome Document 38-2201950-000, "2nd Transmittal of Design Information – Peach Bottom Unit 2", TODI-PEDM-N16A-2, Revision 1.
26. Framatome Document 38-2201953-001, "5th Transmittal of Design Information – Peach Bottom Unit 2", TODI-PEDM-N16A-5, Revision 1.
27. Framatome Document 38-9327939-000, "TODI-11 Transmittal of Design Information Peach Bottom Unit 2."
28. Framatome Document 38-9341324-000, "Exelon Peach Bottom N16A TODI-16", TODI-PEDM-N16A-16.
29. ANSYS Finite Element Computer Code, Version 19.2, ANSYS Inc., Canonsburg, PA.

Attachment 7

"Peach Bottom Unit 2 RV Instrument Nozzle N16A Repair Weld Residual Stress Analysis – Non Proprietary" Framatome Document No. 32-9337544-000, Non-Proprietary Version framatome

CALCULATION SUMMARY SHEET (CSS)

Document No. 32 - 9337544 - 000

Safety Related: ☒Yes ☐ No

Title: Peach Bottom Unit 2 RV Instrument Nozzle N16A Repair Weld Residual Stress Analysis – Non Proprietary

PURPOSE AND SUMMARY OF RESULTS

Purpose: The purpose of this report is to document the results of the weld residual stress finite element analysis of the Reactor Vessel (RV) instrument nozzle N16A penetration as-left J-groove weld at Peach Bottom Unit 2 Nuclear Power Plant. This analysis includes weld simulation of the original J-groove weld attaching the original instrument nozzle to the RV shell, and simulation of the recent weld repair involving outer diameter weld pad and J-groove weld of the replacement nozzle. The state of residual stress at the end of the final welding step, as determined by the ANSYS finite element analysis, is summarized to support subsequent flaw evaluations of the as-left (original) J-groove weld.

Summary of Results: The state of residual stress at the end of the final welding step after shakedown, as determined by the ANSYS finite element analysis are extracted and provided in the ANSYS files reported in Table 5-1 to support the subsequent flaw evaluation of the as-left J-groove weld. See Section 7.0 for a presentation of results.

The proprietary version of this document is 32-9334548-000.

If the computer software used herein is not the latest version per the EASI list, AP 0402-01 requires that justification be provided.

THE FOLLOWING COMPUTER CODES HAVE BEEN USED IN THIS DOCUMENT:

CODE/VERSION/REV	CODE/VERSION/REV
ANSYS v 19.2	

THE DOCUMENT CONTAINS ASSUMPTIONS THAT SHALL BE VERIFIED PRIOR TO USE

☐Yes

☒ No

Review Method: ☒ Design Review (Detailed Check)

☐ Alternate Calculation

Does this document establish design or technical requirements? ☐ YES ☒ NO

Does this document contain Customer Required Format? ☐ YES ☒ NO

Signature Block

Name and Title (printed or typed)	Signature	P/R/A/M and LP/LR	Date	Pages/Sections Prepared/Reviewed/Approved
Jennifer A. Nelson Principal Engineer	*JA NELSON 10/12/2021*	P		All
Ashok Nana Advisory Engineer	*AD NANA 10/13/2021*	M		All
Luziana Matte Technical Consultant Engineer	*LR MATTE 10/13/2021*	R		All
Ryan Hosler Supervisory Engineer	*RS HOSLER 10/13/2021*	A		All

Notes: P/R/A designates Preparer (P), Reviewer ®, Approver (A);
LP/LR designates Lead Preparer (LP), Lead Reviewer (LR);
M designates Mentor (M)

In preparing, reviewing and approving revisions, the lead preparer/reviewer/approver shall use ‘All’ or ‘All except ___’ in the pages/sections reviewed/approved. ‘All’ or ‘All except ___’ means that the changes and the effect of the changes on the entire document have been prepared/reviewed/approved. It does not mean that the lead preparer/reviewer/approver has prepared/reviewed/approved all the pages of the document.

With Approver permission, calculations may be revised without using the latest CSS form. This deviation is permitted when expediency and/or cost are a factor. Approver shall add a comment in the right-most column that acknowledges and justifies this deviation.

Project Manager Approval of Customer References and/or Customer Formatting (N/A if not applicable)

Name (printed or typed)	Title (printed or typed)	Signature	Date	Comments
N/A	N/A	N/A	N/A	N/A

Record of Revision

Revision No.	Pages/Sections/Paragraphs Changed	Brief Description / Change Authorization
000	All	Original Release

Table of Contents

List of Tables

List of Figures

1.0 INTRODUCTION

The purpose of this calculation is to perform a weld residual stress (WRS) finite element analysis of the RV instrument nozzle N16A as-left J-groove weld at Peach Bottom Unit 2 Nuclear Power Plant. This analysis includes weld simulation of the original J-groove weld (JGW) attaching the N16A instrument nozzle to the reactor vessel (RV) shell, simulation of the recent repair involving an outer diameter weld pad (WP) and new J-groove weld (NJGW) attaching the replacement (new) nozzle to the WP. As shown in Reference [1], the repair process involves removing the outer portion of the original nozzle, welding a WP at the outer diameter of the RV shell, and welding of the replacement nozzle to the WP. The final state of stress as predicted by the ANSYS finite element analysis (FEA) at the end of the welding steps is provided in this report to support the subsequent fracture mechanics evaluation of a postulated flaw in the as-left J-groove weld.

2.0 METHODOLOGY

The methodology used to perform the WRS FEA is consistent with the methods described in the WRS analysis procedure (Reference [2]) and with the general recommendations of industry WRS modeling guidance documents such as MRP-317 (Reference [6]). The stages of the welding processes are simulated using a [ ] finite element model (FEM) following the applicable steps defined in the repair implementation drawing (Reference [1]), as detailed below:

1. Develop [ ] FEM [ ]
2. Define design inputs and boundary conditions:
    a. Temperature range for melting (solidus and liquidus temperatures).
    b. Thermal and mechanical temperature dependent material properties from ambient conditions (70°F) up to and including the melting region.
    c. Thermal and structural boundary conditions.
    d. Volumetric heat sources from welding input parameters.
3. Simulate welding of the original JGW, connecting the original nozzle to RV shell using weld material as follows (steps a & b). This step represents the original N16A nozzle configuration (‘Configuration 1’) shown in Figure 6-3.

[ ]

[ ]

4. Simulation of post-weld heat treatment (PWHT) by heating the components of the original configuration to [ ]

5. Static Analysis: Apply static load steps to simulate [ ] Hydrostatic Test followed by [ ]

6. Simulate the start of the N16A nozzle repair, by severing the original nozzle above the head [ ] and simulate welding of WP [ ] This step is shown in Figure 6-4, designated as 'Configuration 2.'

7. Simulate severing the original nozzle to the final configuration and the overbore of the RV shell [ ] and simulate welding the NJGW connecting the new nozzle to WP, [ ] This step is shown in Figure 6-5, designated as 'Configuration 3.'

8. Static Analysis: Apply static load steps to simulate [ ] Steady State operating conditions [ ]

9. The weld residual stresses applicable for subsequent evaluation of a postulated remnant flaw in the as-left J-groove weld are extracted [ ]

3.0 ASSUMPTIONS

3.1 Unverified Assumption

There are no unverified assumptions used in this analysis.

3.2 Justified Assumptions and Modeling Simplifications

The following justified assumptions and modeling simplifications are used in this analysis:

[ ]

[ ]

[ ]

4.0 DESIGN INPUTS

4.1 Geometry

The N16A instrument nozzle geometry for the original and repair configurations are obtained from References [1], [7], [8] and [9], with key dimensions listed in Table 4-1. Figure 4-1 shows the original and repair configurations.

Table 4-1: Key Dimensions

Dimension	Equation	Value	Unit	Reference
Radius to Base Metal	R_s		in	[1], Step 1
Reactor Vessel Wall Thickness (min)	t_s		in	[1], Step 1
Cladding Thickness (nominal)	t_c		in	[7], Part 1, Page 673
Inside Diameter of Original Nozzle	ID_{ON}		in	[1], Step 1
Outside Diameter of Original Nozzle	OD_{ON}		in	[1], Step 1
Depth of Original JGW (from cladding)	H_{JGW}		in	[7], Part 1, Page 673
Diameter of Bore at J-Groove Weld	D_B		in	[1], Step 1
As-Built Weld Pad Thickness (average, M2)	t_{WP}		in	[1], Step 4 [8], Page 45 of 308
As-Built Overbore Diameter (close to bottom)	D_{OB}		in	[1], Step 5.4 [8], Page 129 of 308
As-Built Overbore Depth (M8)	H_{OB}		in	
Inside Diameter of Replacement Nozzle (Small)	ID_{NNS}		in	[9] [8], Page 130 of 308
Inside Diameter of Replacement Nozzle (Large)	ID_{NNL}		in	
Outside Diameter of Replacement Nozzle	OD_{NN}		in	
NJGW Width/Depth into WP	W_{NJGW}		in	[1], Step 5.4

Note(s):

(1) [ ]

[ ]

Figure 4-1: Original and Repair Geometry

4.2 Material

Table 4-2 provides the material designations of the components modeled in the WRS analysis.

Table 4-2: Material Designation

Component	Material Designation	Reference
RV Shell	[	[3]
Cladding		[7]
Original JGW		[1]
Original Nozzle		[3]
Replacement (New) Nozzle		[3]
Weld Pad and NJGW	]	[3]

Note(s):

(1) [

]

Physical material properties (thermal conductivity, specific heat, mean coefficient of thermal expansion, density, Young's modulus, and Poisson's ratio) and stress-strain curves are taken from Reference [11] that are representative of the component materials listed in Table 4-2. [

]

[

]

4.3 Welding Parameters

The welding parameters used in the FEA are listed in Table 4-3.

Table 4-3: Welding Parameters

Weld	Welding Parameter	Value	Unit	Reference
JGW				
Weld Pad				
New JGW				

Note(s):

(1) Per Section 3.2, Item 8.

(2) Per Section 3.2, Item 9.

4.4 Post Weld Heat Treatment Parameters

Post weld heat treatment (PWHT) is applied to the FEM after the JGW simulation per Section 2.0, Item 4. The PWHT parameters applied to the FEM are listed in Table 4-4. In addition, see Section 3.2, Item 6.

Table 4-4: Post Weld Heat Treatment Parameters

Parameter	Value	Unit	Reference
Temperature	[ ]	°F	[ ]
Duration	[ ]	hr	[ ]
Heatup/Cooldown Rate	[ ]	°F/hr	[ ]

Note(s):

[ ]

4.5 Hydrotest and Steady State Operating Conditions

Hydrostatic test and steady state operating conditions are applied to the FEM per Section 2.0, Item 5, which are listed in Table 4-5.

Table 4-5: Hydrotest and Steady State Operating Conditions

Parameter	Value	Unit	Reference
Hydrotest Temperature	[	°F	[
Hydrotest Pressure		psig	
Operating Temperature		°F	
Operating Pressure	]	psig	]

5.0 COMPUTER USAGE

5.1 Hardware / Software

[ ]

Results of the calculations confirm that the inputs and structural responses of the models developed are within the range of applicability of ANSYS Mechanical Enterprise for these types of physical problems.

[ ]

5.2 Computer Files

Table 5-1 lists the computer files and location in the ColdStor directory.

Table 5-1: Computer Files

[/][cold]/[General-Access]/[32]/[32-9000000]/[32-9334548-000]/[official]/[00_ModelData]/

Name	Size	Date/Time Modified	CRC

[/][cold]/[General-Access]/[32]/[32-9000000]/[32-9334548-000]/[official]/[01_WRSAnalysis]/

Name	Size	Date/Time Modified	CRC

6.0 ANALYSIS

6.1 Finite Element Model

[

] Figure 6-2 shows the flow chart of the overall analysis sequence with corresponding input filenames. [ ] The FEM configurations [ ] are shown in Figure 6-3 through Figure 6-5. [ ] Temperature dependent material properties from the weld materials data base from Reference [11] are assigned per Section 4.2. See Section 3.2 for modeling simplifications used to develop the FEM.

[ ]

Figure 6-1: Finite Element Model - Combined Configuration

Figure 6-2: Simulation Flow Chart

[ ]

Figure 6-3: Configuration 1 - JGW Simulation

[ ]

Figure 6-4: Configuration 2 - WP Simulation

[

]

Figure 6-5: Configuration 3 - NJGW Simulation

[

]

6.2 Finite Element Model Boundary Conditions

6.2.1 Thermal Analysis

For the thermal welding simulations of the JGW, WP and NJGW [

]

6.2.2 Structural Analysis

For all structural simulations, [

]

For the structural welding simulations of the JGW, WP and NJGW [

]

Following the JGW analysis, PWHT is simulated [

]

After the PWHT analysis, [ ] hydro tests are simulated followed by [ ] steady state operating conditions using the temperature and pressure values specified in Table 4-5 [ ] In addition, [ ] steady state operating conditions using the temperature and pressure values specified in Table 4-5 [ ] are applied after the NJGW analysis. [

]

[ ]

7.0 SUMMARY OF RESULTS

The final state of stresses in the Peach Bottom Unit 2 RV N16A instrument nozzle following the WRS FEA are [ ] These results are to be used in the subsequent flaw evaluation of the as-left (original) J-groove weld.

Figure 7-1 and Figure 7-2 present the axial and hoop stress contours at cold conditions following the completion of hydrostatic test and operating condition cycles on the initial configuration (see Figure 6-3). Figure 7-3 and Figure 7-4 present the axial and hoop stress contours for the final stress state following completion of operating conditions cycles on the final repair configuration (see Figure 6-5). The stress-contours are presented in cylindrical coordinate systems that are aligned with the axis of the nozzle, where 'Z' is axial and 'Y' is hoop. The unit of stress is in psi.

[ ]

The weld residual stresses applicable for evaluating a postulated remnant flaw in the as-left J-groove weld are extracted [ ]

[ ]

Figure 7-1: Distribution of Residual Axial Stress (SZ): Post Hydrotest and Operating at 70°F (psi) – Original Configuration

[ ]

Figure 7-2: Distribution of Residual Hoop Stress (SY): Post Hydrotest and Operating at 70°F (psi) – Original Configuration

[ ]

Figure 7-3: Distribution of Residual Axial Stress (SZ): Final Stress State Post Operating Cycles at 70°F (psi) – Final Repair Configuration

[ ]

Figure 7-4: Distribution of Residual Hoop Stress (SY): Final Stress State Post Operating Cycles at 70°F (psi) – Final Repair Configuration

Figure 7-5: [ ] Nodes for Stress Extraction

Figure 7-6: [ ] Nodes for Stress Extraction

8.0 REFERENCES

1. Framatome Drawing 02-8124069E-002, "Peach Bottom Unit 2 N16A Nozzle Replacement Implementation."
2. Framatome Document 32-2500013-001, "Technical Basis for Numerical Simulation of Welding Residual Stresses."
3. Framatome Document 08-9320930-002, "Peach Bottom Unit 2 N16A Instrumentation Nozzle Replacement – Design Specification."
4. Framatome Document 32-2500062-001, "Creep Material Properties for Welding Residual Stress Analysis Including PWHT."
5. Framatome Document 38-9327939-000, "TODI-11 Transmittal of Design Information Peach Bottom Unit 2."
6. Materials Reliability Program: Welding Residual Stress Dissimilar Metal Butt-Weld Finite Element Modeling Handbook (MRP-317, Revision 1). EPRI, Palo Alto, CA: 2015. 3002005499.
7. Framatome Document 38-2201949-000, "1st Transmittal of Design Information – Peach Bottom Unit 2," TODI-PEDM-N16A-1, Revision 0.
8. Framatome Document 50-9320938-000, "Completed Traveler – Peach Bottom 2, N16A Nozzle Repair During P2R23."
9. Framatome Drawing 02-9180866C-003, "2 Inch Instrumentation Replacement Nozzle."
10. Framatome Condition Report CR-2020-2586.
11. Framatome Document 32-2500012-002, "Materials Database for Weld Residual Stress Finite Element Analyses."
12. ANSYS Finite Element Computer Code, Version 19.2, ANSYS Inc., Canonsburg, PA.
13. Framatome Document 55-WP3-43-F43TBSCa3-009, "Welding Procedure Specification."
14. Framatome Document 55-WP43-43-F43AW1-001, "Welding Procedure Specification."
15. ASME Boiler and Pressure Vessel Code, Section III, 1965 with Addenda to Winter 1965.
16. Framatome Document 38-2201951-000, "3rd Transmittal of Design Information – Peach Bottom Unit 2," TODI-PEDM-N16A-3, Revision 0.

Attachment 8

"Corrosion Evaluation of the Peach Bottom Unit 2 N16-A Reactor Vessel Nozzle Modification – Non Proprietary," Framatome Document No. 51- 9321006-002, Non-Proprietary Version

Framatome Inc.

Engineering Information Record

Document No.: 51 - 9321006 - 002

Corrosion Evaluation of the Peach Bottom Unit 2 N16-A Reactor Vessel Nozzle Modification – Non Proprietary

Safety Related? ☒ YES ☐ NO

Does this document establish design or technical requirements? ☐ YES ☒ NO

Does this document contain assumptions requiring verification? ☐ YES ☒ NO

Does this document contain Customer Required Format? ☐ YES ☒ NO

Signature Block

Name and Title/Discipline	Signature	P/LP, R/LR, M, A-CRF, A	Date	Pages/Sections Prepared/Reviewed/ Approved or Comments
Roluf Andersen Engineer I Materials Engineering	*RB ANDERSEN* *12/10/2021*	P		All
Ryan Hosler Supervisory Engineer Materials Engineering	*RS HOSLER* *12/10/2021*	R		All
Darren Wood Manager IBPE-Engineering	*DH WOOD* *12/10/2021*	A		All

Note: P/LP designates Preparer (P), Lead Preparer (LP)
M designates Mentor (M)
R/LR designates Reviewer (R), Lead Reviewer (LR)
A-CRF designates Project Manager Approver of Customer Required Format (A-CRF)
A designates Approver/RTM – Verification of Reviewer Independence

Project Manager Approval of Customer References (N/A if not applicable)

Name (printed or typed)	Title (printed or typed)	Signature	Date
David Skulina	Project Manager	*DJ SKULINA* *12/10/2021*	

Project Manager signature above indicates the applicable IBPE approval of Reference 5.

Record of Revision

Revision No.	Pages/Sections/ Paragraphs Changed	Brief Description / Change Authorization
000	All	Original release (November 2020).
		The Proprietary version of this document is 51-9320932-000.
001	See Description	References 6 and 13 added and remaining references renumbered appropriately. Added wording to Section 5.0 to provide clarification on results of subsequent analyses. Minor wording changes made in Section 3.4.
		The Proprietary version of this document is 51-9320932-001.
002	See Description	Additional discussion added to Section 3.4. All references to “one operating cycle” updated to “life of the repair”. Added Reference 11. Updated References 1, 6, and 14.
		The Proprietary version of this document is 51-9320932-002.

Table of Contents

List of Figures

Page

1.0 PURPOSE

The repair of the N16-A reactor vessel nozzle in the Peach Bottom Unit 2 reactor vessel will change the penetration configuration in the following ways: 1) the repair exposes the low alloy steel (LAS) reactor vessel to water conditions, 2) the repair includes a new Alloy 690 nozzle as part of the pressure boundary, and 3) the repair includes a new Alloy 52M weld pad and partial penetration J-groove weld as part of the pressure boundary (References 1 and 2). Also, the reducing coupling to nozzle weld is now an Alloy 52M dissimilar metal weld. The original configuration and the final repair configuration, as well as materials, are shown in Figure 1-1 and Figure 1-2 respectively.

The following corrosion evaluation considers potential material degradation due to each of these changes. Information contained in bold brackets in this document is considered Proprietary to Framatome.

Figure 1-1: Original Configuration (Shown with Sealing Plug in Place) (References 1 and 2)

Figure 1-2: Final Repair Configuration (Shown with Sealing Plug in Place) (References 1 and 2)

2.0 ASSUMPTIONS

2.1 Assumptions Requiring Verification

[ ]

2.2 Justified Assumptions

[ ]

3.0 CORROSION OF EXPOSED LOW ALLOY STEEL

The LAS reactor vessel material exposed due to the repair, as shown in red in Figure 1-2, will be in the water space environment given the elevation of the N16-A nozzle (Reference 1). The requirements of the Reactor Water Chemistry control program for Peach Bottom are based on BWRVIP-190, Revision 1 (References 3 and 4).

3.1 General Corrosion

Due to the repair configuration, a small portion of the LAS reactor vessel material will be openly exposed to boiling water reactor (BWR) water and, thus, general corrosion is considered. [

]

[ ]

3.2 Galvanic Corrosion

[ ]

3.3 Crevice Corrosion

[ ] The environmental conditions in a crevice can become aggressive with time and can cause accelerated local corrosion.

[ ]

3.4 Stress Corrosion Cracking

[ ]

Although it is very unlikely that SCC cracks will initiate and propagate in LAS under normal BWR conditions, it is impossible to completely rule out. Hence, it is prudent to examine the feasibility of performing an allowable flaw evaluation for an assumed flaw propagating from the J-groove weld into the LAS by applying the American Society of Mechanical Engineers (ASME) Boiler and Pressure Vessel (B&PV) Code Section XI criteria (Reference 10). [ ]

[ ]

[ ]

- As noted in Section 3.0, requirements of the Reactor Water Chemistry control program for Peach Bottom are based on BWRVIP-190, Revision 1. See Section 2.2 for Justified Assumption 1 for additional details regarding [ ]
- [ ]
- [ ]

[ ]

Figure 3-1: [ ]

This CGR equation/curve was used to support the ASME Section XI analysis (Reference 14), which concluded that the postulated flaw is acceptable for the life of the repair.

4.0 CORROSION OF ALLOY 690 AND ALLOY 52M

Stress corrosion cracking failures of Alloy 600 and its associated weld metals (Alloy 82/182) have occurred in domestic and international light water reactors. The BWR industry addressed this issue by replacing or modifying affected materials with a modified version of Alloy 600 and Alloy 82/182 (Reference 15). The modified Alloy 82/182 added carbide stabilizers (niobium and tantalum) to minimize chromium depletion at the grain boundaries. The pressurized water reactor (PWR) industry selected Alloy 690 and Alloy 52/152 as replacement materials (Reference 16). Alloy 690 was also thermally treated to improve the microstructure, but grain boundary chromium depletion of Alloy 690/52/152 was avoided by doubling the chromium content (from ~15% to ~30%) instead of using carbide stabilizers. Laboratory studies indicate that Alloy 690 and Alloy 52/152 have superior SCC resistance relative to the non-modified Alloy 600 and Alloy 82/182 (Reference 16).

Although most testing of Alloy 690/52/152 has been under PWR conditions, some studies have been performed in environments more similar to BWRs. Creviced U-bend specimens of Alloy 600 and Alloy 690 were tested at 600°F for 48 weeks with an environment of 6 ppm oxygen (Reference 17). The Alloy 600 readily cracked, whereas Alloy 690 showed no cracking. Also, testing of Alloy 690 in high purity water containing 36 ppm oxygen at 289°C (~550°F) for 47 weeks resulted in no cracking (Reference 17).

Extensive testing has been performed on Alloy 52/152 in high temperature deaerated water, which indicate that Alloy 52/152 is much less susceptible to SCC compared to Alloy 82/182 (the Alloy 600 weld metal) (References 16, 18, and 19). Test data of Alloy 52/152 in a high temperature oxygenated environment is not readily available, but Alloy 52/152 is expected to have a low susceptibility to SCC under these conditions as well based on the similarity of Alloy 52/152 to Alloy 690.

The only difference between the Alloy 52M to be used in the repair and Alloy 52/152 are small alloying additions to improve weldability. The corrosion resistance is expected to be similar. Based on laboratory studies and operating experience, the replacement higher chromium content nickel-based alloys (Alloy 690 and Alloy 52M) are much less susceptible to SCC than Alloy 600 and Alloy 182 and SCC of these materials is not expected during the life of the modification.

5.0 CONCLUSION

The modification of the N16-A reactor vessel nozzle at Peach Bottom exposes the LAS reactor vessel in a small area to a water environment and introduces new materials (Alloy 690 and Alloy 52M). For the exposed LAS, general corrosion, galvanic corrosion, crevice corrosion, and SCC were evaluated. It is concluded that 1) galvanic corrosion and crevice corrosion are bound by general corrosion, 2) the projected material loss by general corrosion is not a concern for the life of the repair based on the Section III analysis, and 3) SCC is not a concern for the life of the repair based on the Section XI analysis. In addition, it is concluded that SCC of the replacement higher chromium content nickel-based alloys (Alloy 690 and Alloy 52M) is not a concern over the life of the modification.

6.0 REFERENCES

References identified with an (*) are maintained within Exelon Records System and are not retrievable from Framatome Records Management. These are acceptable references per Framatome Administrative Procedure 0402-01, Attachment 7. See page 2 for Project Manager Approval of customer references.

1. **[ ]**
2. **[ ]**
3. **BWRVIP-190 Revision 1: BWR Vessel and Internals Project, Volume 2: BWR Water Chemistry Guidelines - Technical Basis. EPRI, Palo Alto, CA: 2014. 3002002623.*
4. **[ ]**
5. **[ ]**
6. **[ ]**
7. ASM Handbook, Volume 13, "Corrosion", Formerly 9th Edition, Metals Handbook.
8. D.C. Vreeland, et al., "Corrosion of Carbon and Low-Alloy Steels in Out-of-Pile Boiling-Water-Reactor Environment," Corrosion, Vol 17, No. 6, 1961.
9. **[ ]**
10. ASME B&PV Code, Section XI, Rules for Inservice Inspection of Nuclear Power Plant Components, Division 1, 2013 Edition, Subject to the conditions of 10 CFR 50.55a.
11. H. P. Seifert and S. Ritter, "New Observations about the SCC Crack Growth Behavior of Low-Alloy RPV Steels under BWR/NWC Conditions," 11th International Conference on Environmental Degradation of Materials in Nuclear Power Systems, Aug 10-14, 2003, Stevenson, WA, ANS.
12. **[ ]**
13. **[ ]**
14. **[ ]**
15. NUREG/CR-6923, "Expert Panel Report on Proactive Materials Degradation Assessment."

16. Materials Reliability Program (MRP): Resistance to Primary Water Stress Corrosion Cracking of Alloys 690, 52, and 152 in Pressurized Water Reactors (MRP-111). EPRI, Palo Alto, CA: 2004. 1009801.

17. Sedriks, A.J., Schultz, J.W., Cordovi, M.A., "Inconel Alloy 690 – A New Corrosion Resistant Material," Corrosion Engineering (Boshoku Gijutsu), vol. 28, pp. 82-95, 1979, Japan Society of Corrosion Engineering.

18. M. J. Psaila-Dombrowski et al., "Evaluation of Weld Metals 82, 152, 52 and Alloy 690 Stress Corrosion Cracking and Corrosion Fatigue Susceptibility," Eighth International Symposium on Environmental Degradation of Materials in Nuclear Power Systems – Water Reactors, Aug 10-14 1997, Amelia Island, FL, ANS.

19. Crum, J.R., Nagashima, T., "Review of Alloy 690 Steam Generator Studies," Eight International Symposium on Environmental Degradation of Materials In Nuclear Power Systems – Water Reactors, Aug 10-14 1997, Amelia Island, FL, ANS.

Attachment 9

Affidavit Associated with Framatome Document No. 32-9335342-000

A F F I D A V I T

1. My name is Gayle Elliott. I am Deputy Director, Licensing and Regulatory Affairs, for Framatome Inc. (Framatome) and as such I am authorized to execute this Affidavit.

2. I am familiar with the criteria applied by Framatome to determine whether certain Framatome information is proprietary. I am familiar with the policies established by Framatome to ensure the proper application of these criteria.

3. I am familiar with the Framatome information contained in Calculation Summary Sheet 32-9335342-000 entitled "Peach Bottom Unit 2 RV instrument Nozzle N16A Repair As-Left J-Groove Weld Analysis," dated December 10, 2021 and referred to herein as "Document." Information contained in this Document has been classified by Framatome as proprietary in accordance with the policies established by Framatome for the control and protection of proprietary and confidential information.

4. This Document contains information of a proprietary and confidential nature and is of the type customarily held in confidence by Framatome and not made available to the public. Based on my experience, I am aware that other companies regard information of the kind contained in this Document as proprietary and confidential.

5. This Document has been made available to the U.S. Nuclear Regulatory Commission in confidence with the request that the information contained in this Document be withheld from public disclosure. The request for withholding of proprietary information is made in accordance with 10 CFR 2.390. The information for which withholding from disclosure is requested qualifies under 10 CFR 2.390(a)(4) "Trade secrets and commercial or financial information."

6. The following criteria are customarily applied by Framatome to determine whether information should be classified as proprietary:

(a) The information reveals details of Framatome's research and development plans and programs or their results.

(b) Use of the information by a competitor would permit the competitor to significantly reduce its expenditures, in time or resources, to design, produce, or market a similar product or service.

(c) The information includes test data or analytical techniques concerning a process, methodology, or component, the application of which results in a competitive advantage for Framatome.

(d) The information reveals certain distinguishing aspects of a process, methodology, or component, the exclusive use of which provides a competitive advantage for Framatome in product optimization or marketability.

(e) The information is vital to a competitive advantage held by Framatome, would be helpful to competitors to Framatome, and would likely cause substantial harm to the competitive position of Framatome.

The information in this Document is considered proprietary for the reasons set forth in paragraphs 6(d) and 6(e) above.

7. In accordance with Framatome's policies governing the protection and control of information, proprietary information contained in this Document has been made available, on a limited basis, to others outside Framatome only as required and under suitable agreement providing for nondisclosure and limited use of the information.

8. Framatome policy requires that proprietary information be kept in a secured file or area and distributed on a need-to-know basis.

9. The foregoing statements are true and correct to the best of my knowledge, information, and belief.

I declare under penalty of perjury that the foregoing is true and correct.

Executed on: December 10, 2021.

ELLIOTT Gayle
Digitally signed by ELLIOTT Gayle
Date: 2021.12.10 15:29:00 -05'00'

Gayle Elliott

Attachment 10

Affidavit Associated with Framatome Document No. 32-9334548-000

A F F I D A V I T

1. My name is Philip A. Opsal. I am Manager, Product Licensing for Framatome Inc. (formally known as AREVA Inc.), and as such I am authorized to execute this Affidavit.

2. I am familiar with the criteria applied by Framatome to determine whether certain Framatome information is proprietary. I am familiar with the policies established by Framatome to ensure the proper application of these criteria.

3. I am familiar with the Framatome information contained in Framatome Calculation Summary Sheet 32-9334548-000 Title: “Peach Bottom Unit 2 RV Instrumentation Nozzle N16A Repair Weld Residual Stress Analysis.” Information contained in this Document has been classified by Framatome as proprietary in accordance with the policies established by Framatome for the control and protection of proprietary and confidential information.

4. This Document contains information of a proprietary and confidential nature and is of the type customarily held in confidence by Framatome and not made available to the public. Based on my experience, I am aware that other companies regard information of the kind contained in this Document as proprietary and confidential.

5. This Document has been made available to the U.S. Nuclear Regulatory Commission in confidence with the request that the information contained in this Document be withheld from public disclosure. The request for withholding of proprietary information is made in accordance with 10 CFR 2.390. The information for which withholding from disclosure is requested qualifies under 10 CFR 2.390(a)(4) “Trade secrets and commercial or financial information.”

6. The following criteria are customarily applied by Framatome to determine whether information should be classified as proprietary:

(a) The information reveals details of Framatome’s research and development plans and programs or their results.

(b) Use of the information by a competitor would permit the competitor to significantly reduce its expenditures, in time or resources, to design, produce, or market a similar product or service.

(c) The information includes test data or analytical techniques concerning a process, methodology, or component, the application of which results in a competitive advantage for Framatome.

(d) The information reveals certain distinguishing aspects of a process, methodology, or component, the exclusive use of which provides a competitive advantage for Framatome in product optimization or marketability.

(e) The information is vital to a competitive advantage held by Framatome, would be helpful to competitors to Framatome, and would likely cause substantial harm to the competitive position of Framatome.

The information in this Document is considered proprietary for the reasons set forth in paragraphs 6(b), 6 (c), and 6(e) above.

7. In accordance with Framatome’s policies governing the protection and control of information, proprietary information contained in this Document has been made available, on a limited basis, to others outside Framatome only as required and under suitable agreement providing for nondisclosure and limited use of the information.

8. Framatome policy requires that proprietary information be kept in a secured file or area and distributed on a need-to-know basis.

9. The foregoing statements are true and correct to the best of my knowledge, information, and belief.

I declare under penalty of perjury that the foregoing is true and correct.

Executed on October 13, 2021.

Philip A. Opsal

Attachment 11

Affidavit Associated with Framatome Document No. 51-9320932-002

A F F I D A V I T

1. My name is Gayle Elliott. I am Deputy Director, Licensing and Regulatory Affairs, for Framatome Inc. (Framatome) and as such I am authorized to execute this Affidavit.

2. I am familiar with the criteria applied by Framatome to determine whether certain Framatome information is proprietary. I am familiar with the policies established by Framatome to ensure the proper application of these criteria.

3. I am familiar with the Framatome information contained in Engineering Information Record 51-9320932-002 entitled "Corrosion Evaluation of the Peach Bottom Unit 2 N16-A Reactor Vessel Nozzle Modification," dated December 10, 2021 and referred to herein as "Document." Information contained in this Document has been classified by Framatome as proprietary in accordance with the policies established by Framatome for the control and protection of proprietary and confidential information.

4. This Document contains information of a proprietary and confidential nature and is of the type customarily held in confidence by Framatome and not made available to the public. Based on my experience, I am aware that other companies regard information of the kind contained in this Document as proprietary and confidential.

5. This Document has been made available to the U.S. Nuclear Regulatory Commission in confidence with the request that the information contained in this Document be withheld from public disclosure. The request for withholding of proprietary information is made in accordance with 10 CFR 2.390. The information for which withholding from disclosure is requested qualifies under 10 CFR 2.390(a)(4) "Trade secrets and commercial or financial information."

6. The following criteria are customarily applied by Framatome to determine whether information should be classified as proprietary:

(a) The information reveals details of Framatome's research and development plans and programs or their results.

(b) Use of the information by a competitor would permit the competitor to significantly reduce its expenditures, in time or resources, to design, produce, or market a similar product or service.

(c) The information includes test data or analytical techniques concerning a process, methodology, or component, the application of which results in a competitive advantage for Framatome.

(d) The information reveals certain distinguishing aspects of a process, methodology, or component, the exclusive use of which provides a competitive advantage for Framatome in product optimization or marketability.

(e) The information is vital to a competitive advantage held by Framatome, would be helpful to competitors to Framatome, and would likely cause substantial harm to the competitive position of Framatome.

The information in this Document is considered proprietary for the reasons set forth in paragraphs 6(d) and 6(e) above.

7. In accordance with Framatome's policies governing the protection and control of information, proprietary information contained in this Document has been made available, on a limited basis, to others outside Framatome only as required and under suitable agreement providing for nondisclosure and limited use of the information.

8. Framatome policy requires that proprietary information be kept in a secured file or area and distributed on a need-to-know basis.

9. The foregoing statements are true and correct to the best of my knowledge, information, and belief.

I declare under penalty of perjury that the foregoing is true and correct.

Executed on: December 10, 2021.

ELLIOTT Gayle Digitally signed by ELLIOTT Gayle
Date: 2021.12.10 16:17:02 -05'00'

Gayle Elliott